Synaptically activated Ca^{2+} waves and NMDA spikes locally suppress voltage dependent Ca^{2+} signaling in rat pyramidal cell dendrites

Satoshi Manita[1,2], Kenichi Miyazaki[1,2], and William N. Ross[1,2]

[1]Department of Physiology, New York Medical College, Valhalla, NY 10595

[2]Marine Biological Laboratory, Woods Hole, MA 02543

Running title: Local suppression of Ca^{2+} signaling in dendrites

Keywords: dendrite, calcium, pyramidal neuron

Words in manuscript: 6752

Corresponding Author:

Dr. William Ross

Department of Physiology

New York Medical College

Valhalla, NY 10595

Email: ross@nymc.edu

Table of contents category: Neuroscience

Non-technical summary Synaptically activated changes in dendritic $[Ca^{2+}]_i$ affect many important physiological processes including synaptic plasticity and gene expression. The location, magnitude, and time course of these changes can determine which mechanisms are affected. Therefore, it is important to understand the processes that control and modulate these changes. One important source is Ca^{2+} entering through voltage gated Ca^{2+} channels opened by action potentials backpropagating over the dendrites (bAPs). Here we examine how $[Ca^{2+}]_i$ changes, caused by regenerative Ca^{2+} release from internal stores (Ca^{2+} waves) or by regenerative Ca^{2+} entry through NMDA receptors (NMDA spikes) affect subsequent bAP evoked $[Ca^{2+}]_i$ changes. These large $[Ca^{2+}]_i$ increases suppressed the bAP signals in the regions where the preceding $[Ca^{2+}]_i$ increases were largest. The suppression was proportional to the magnitude of the large $[Ca^{2+}]_i$ change and was insensitive to kinase and phosphatase inhibitors, consistent with suppression due to Ca^{2+} dependent inhibition of Ca^{2+} channels.

Abstract

Postsynaptic $[Ca^{2+}]_i$ changes contribute to several kinds of plasticity in pyramidal neurons. We examined the effects of synaptically activated Ca^{2+} waves and NMDA spikes on subsequent Ca^{2+} signaling in CA1 pyramidal cell dendrites in hippocampal slices. Tetanic synaptic stimulation evoked a localized Ca^{2+} wave in the primary apical dendrites. The $[Ca^{2+}]_i$ increase from a backpropagating action potential (bAP) or subthreshold depolarization was reduced if it was generated immediately after the wave. The suppression had a recovery time of 30-60s. The suppression only occurred where the wave was generated and was not due to a change in bAP amplitude or shape. The suppression also could be generated by Ca^{2+} waves evoked by uncaging IP_3, showing that other signaling pathways activated by the synaptic tetanus were not required. The suppression was proportional to the amplitude of the $[Ca^{2+}]_i$ change of the Ca^{2+} wave and was not blocked by a spectrum of kinase or phosphatase inhibitors, consistent with suppression due to Ca^{2+} dependent inactivation of Ca^{2+} channels. The waves also reduced the frequency and amplitude of spontaneous, localized Ca^{2+} release events in the dendrites by a different mechanism, probably by depleting the stores at the site of wave generation. The same synaptic tetanus often evoked NMDA spike-mediated $[Ca^{2+}]_i$ increases in the oblique dendrites where Ca^{2+} waves do not propagate. These NMDA spikes suppressed the $[Ca^{2+}]_i$ increase caused by bAPs in those regions. $[Ca^{2+}]_i$ increases by Ca^{2+} entry through voltage-gated Ca^{2+} channels also suppressed the $[Ca^{2+}]_i$ increases from subsequent bAP in regions where the voltage-gated $[Ca^{2+}]_i$ increases were largest, showing that all ways of raising $[Ca^{2+}]_i$ could cause suppression.

Abbreviations bAP, backpropagating action potential; VGCC, voltage-gated calcium channel; ROI, region of interest; CDI, calcium dependent inhibition; Caged IP_3, (D-*myo*-inositol 1,4,5-trisphosphate, $p^{4(5)}$-1-(2-nitrophenyl)ethyl ester; AM251, *N*-(Piperidin-1-yl)-5-(4-iodophenyl) -1-(2,4-dichlorophenyl)-4-methyl-1*H*-pyrazole-3-car boxamide; KN-62, 4-[(2*S*)-2-[(5-isoquinolinylsulfonyl)methylamino]-3-oxo-3-(4-phenyl-1-piperazinyl)propyl] phenyl isoquinolinesulfonic acid ester; H-7, (±)-1-(5-Isoquinolinesulphonyl)-2-methylpiperazine dihydrochloride; W-7, *N*-(6-Aminohexyl)-5-chloro-1-naphthalenesulfonamide hydrochloride; FK-506, (3*S*,4*R*,5*S*,8*R*,9*E*,12*S*,14*S*,15*R*,16*S*,18*R*,19*R*,26a*S*)-,6,8,11,12,13,14,15,16,17,18,19,24,25,26,26a-Hexadecahydro-5,19-dihydroxy-3-[(1*E*)-2-[(1*R*,3*R*,4*R*)-4-hydroxy-3-methoxycyclohexyl]-1-methylethenyl]-14,16-dimethoxy-4,10,12,18-tetramethyl-8-(2-propen-1-yl)-15,19-epoxy-3*H*-pyrido[2,1-*c*][1,4]oxaazacyclotricosine-1,7,20,21(4*H*,23*H*)tetrone.

Introduction

Synaptically activated $[Ca^{2+}]_i$ changes evoke several kinds of plasticity in pyramidal neurons. These include changes in synaptic strength (Malenka & Nicoll, 1999), and changes in electrical properties of the neuron (Frick *et al.* 2004; Kim *et al.* 2007). Important considerations in determining which kinds of plasticity are generated are the location, magnitude, and source of the $[Ca^{2+}]_i$ changes in the cell. Synaptic plasticity primarily results from Ca^{2+} entry into spines through NMDA receptors and the $[Ca^{2+}]_i$ increase is usually localized to the spine head (Sabatini *et al.* 2001). This source of Ca^{2+} is also responsible for some forms of electrical plasticity (Fan *et al.* 2005). Ca^{2+} entry through voltage-gated Ca^{2+} channels (VGCCs) can evoke LTP under some conditions (Grover & Teyler, 1990) and can cause plasticity of spine Ca^{2+} channels (Yasuda *et al.* 2003).

A third source of $[Ca^{2+}]_i$ increase in the dendrites is Ca^{2+} release from intracellular stores, often in the form of large amplitude Ca^{2+} waves (Nakamura *et al.* 1999; Power & Sah, 2007; Hagenston *et al.* 2008) or small localized Ca^{2+} release events (IP_3 receptor-mediated release, "puffs" or ryanodine receptor-mediated release, "sparks;" Manita & Ross, 2009). Ca^{2+} waves primarily occur on the main apical dendrites (Nakamura *et al.* 2002), but sometimes are found near dendritic spines (Holbro *et al.* 2009). There is evidence that Ca^{2+} release from stores participates in some forms of LTP and LTD (Reyes & Stanton, 1996; Taufiq *et al.* 2005; Dudman *et al.* 2007). More directly, Fernández de Sevilla *et al.* (2008) showed that Ca^{2+} waves induce a form of NMDA receptor-independent form of LTP. Holbro *et al.* (2009) showed that localized Ca^{2+} release in some spines and nearby dendrites causes LTD.

A fourth source of dendritic $[Ca^{2+}]_i$ increase are NMDA spikes (Schiller *et al.* 2000; Major *et al.* 2008). These large, spatially restricted $[Ca^{2+}]_i$ increases result from the regenerative activation of NMDA receptors and dendritic Ca^{2+} channels and have been shown to affect LTP in certain regions of pyramidal cell basal dendrites (Gordon *et al.* 2006).

The effects of Ca^{2+} release and NMDA spikes on the electrical and channel properties in dendrites are just beginning to be examined. Topolnik *et al.* (2009) found

that local activation of mGluR5 receptors in hippocampal interneurons induced long-lasting potentiation of action potential evoked Ca^{2+} transients, which required intracellular Ca^{2+} release and PKC activation. Brager & Johnston (2007) found that dendritic h-channels were down regulated following a stimulus protocol that was pharmacologically identified to release Ca^{2+} from intracellular stores.

In our current experiments we examined the effects of large amplitude $[Ca^{2+}]_i$ changes during Ca^{2+} waves and NMDA spikes on the backpropagating action potential (bAP) evoked and subthreshold depolarization evoked $[Ca^{2+}]_i$ changes that immediately followed the wave or spike. The amplitude of these $[Ca^{2+}]_i$ increases was locally suppressed for ~30 - 60 s. The frequency and amplitude of localized Ca^{2+} release events were also suppressed by Ca^{2+} waves, but this suppression primarily occurred through a different mechanism. Since bAP evoked $[Ca^{2+}]_i$ changes themselves contribute to various forms of plasticity these results suggest an additional way that these plastic changes can be locally modulated. The experiments also revealed a complexity in the interactions of Ca^{2+} signaling mechanisms that is essentially invisible to electrical recordings.

Methods

Whole-cell recording and stimulation

Transverse hippocampal slices (300 μm thick) from 5- to 6-week-old Sprague–Dawley rats were prepared as previously described (Nakamura *et al.* 2002). A few experiments examined younger animals (2- to 4-week old) with the same results. Animals were anaesthetized with isoflurane and decapitated using procedures approved by the Institutional Animal Care and Use Committee of New York Medical College. Just before decapitation the heart was perfused with ice cold solution artificial cerebrospinal fluid (ACSF) composed of (mM): 80 NaCl, 2.5 KCl, 0.29 $CaCl_2$, 7 $MgCl_2$, 1.25 NaH_2PO_4, 25 $NaHCO_3$, 75 sucrose, 10.1 glucose, 1.3 ascorbate and 3 pyruvate. Slices were cut in the same solution. They were incubated for at least 1 h in solution consisting of (mM): 124 NaCl, 2.5 KCl, 2 $CaCl_2$, 2 $MgCl_2$, 1.25 NaH_2PO_4, 26 $NaHCO_3$, and 10.1 glucose, 1.3 ascorbate and 3 pyruvate, bubbled with a mixture of 95% O_2–5% CO_2, making the final

pH 7.4. Normal ACSF composed of (mM): 124 NaCl, 2.5 KCl, 2 $CaCl_2$, 2 $MgCl_2$, 1.25 NaH_2PO_4, 26 $NaHCO_3$ and 10.1 glucose, was used for recording.

Submerged slices were placed in a chamber mounted on a stage rigidly bolted to an air table and were viewed with a 40X or 60X water-immersion lens in an Olympus BX50WI microscope mounted on an *X–Y* translation stage. Somatic whole-cell recordings were made using patch pipettes pulled from 1.5 mm outer diameter thick-walled glass tubing (1511-M, Friedrich and Dimmock, Millville, NJ, USA). Tight seals on CA1 pyramidal cell somata were made with the 'blow and seal' technique using video-enhanced DIC optics to visualize the cells (Sakmann & Stuart, 1995). For most experiments the pipette solution contained (mM): 145 potassium gluconate, 4 NaCl, 4 Mg-ATP, 0.3 Na-GTP, 14 Na-phosphocreatine, and 10 Hepes, pH adjusted to 7.3 with KOH. Final osmolarity was 297 mOs. This solution was supplemented with low affinity Ca^{2+} indicators, either 50 μM OGB-1 or 200 μM Oregon Green Bapta-5N (Molecular Probes, Eugene, OR, USA). Synaptic stimulation was evoked with 200 μs pulses with glass electrodes placed on the slice about 5–30 μm to the side of the main apical dendritic shaft and at varying distances from the soma. These electrodes were low resistance patch pipettes (less than 10 MΩ) filled with ACSF. We controlled the amplitude of the synaptic response to be below the threshold for action potential (AP) generation, either by regulating the stimulation current or hyperpolarizing the cell body with the patch electrode on the soma. Temperature in the chamber was maintained between 31 and 33°C, except when temperature was specifically varied. Caged IP_3 (D-*myo*-inositol 1,4,5-trisphosphate, $p^{4(5)}$-1-(2-nitrophenyl)ethyl ester; Walker *et al.* 1987) was purchased from EMD Biosciences (La Jolla, CA). All other chemicals were obtained from Fisher Scientific (Piscataway, NJ, USA), Sigma Chemical Co. (St Louis, MO, USA), or Tocris Bioscience (Ellisville, MO). Stock solutions were prepared (nifedipine,100 mM in DMSO; nimodipine, 10 mM in EtOH; AM251, 2 mM in DMSO; staurosporine, 1 mM in DMSO; KN-62, 4 mM in DMSO; thapsigargin, 5 mM in DMSO; H-7 and W-7, 10 mM in H_20), frozen, and diluted to final concentration in ACSF just before use. For experiments using nifedipine or nimodipine care was taken to minimize exposure to light except in the experimental chamber at the time of the test.

Dynamic $[Ca^{2+}]_i$ measurements

Time-dependent $[Ca^{2+}]_i$ measurements from different regions of the pyramidal neuron were made as previously described (Lasser-Ross *et al.* 1991; Manita & Ross, 2009). Briefly, a RedShirtImaging (Atlanta, GA) NeuroCCD-SMQ cooled CCD camera was mounted on the camera port of the microscope and their Neuroplex software controlled readout parameters and synchronization with electrical recordings. A custom program was used to analyze and display the data. We measured fluorescence changes of OGB-1 and OGB-5N with excitation at 494 ± 10 nm and emission at 536 ± 20 nm. $[Ca^{2+}]_i$ changes are expressed as $\Delta F/F$ where F is the fluorescence intensity when the cell is at rest and ΔF is the change in fluorescence during activity. Corrections were made for indicator bleaching during trials by subtracting the signal measured under the same conditions when the cell was not stimulated. We did not correct for tissue autofluorescence.

To examine the spatial distribution of postsynaptic $[Ca^{2+}]_i$ changes we selected pyramidal neurons that were in the plane of the slice and close to the surface. In these neurons, we could examine $[Ca^{2+}]_i$ increases over a range of 110 μm with the 60X lens and 165 μm with the 40X lens. Increases in different parts of the cell are displayed using either selected regions of interest (ROIs) or a pseudo 'line scan' display (Nakamura *et al.* 2000).

Photolysis of caged IP_3

Caged IP_3 (200-400 μM) was included in the patch pipette, and was allowed to diffuse throughout the cell after membrane rupture. Pulsed UV light centered at 365 nm from a light-emitting diode (UVILED, Rapp Optoelectronics) was focused through the objective via a 200 μm diameter quartz fiber optic light guide making a spot of about 10-15 μm in diameter on the slice with the 60X objective lens. UV light intensity was regulated by changing the fraction of time the UV light was on during a high frequency pulse train (Manita & Ross, 2010).

Results

Suppression by Ca^{2+} waves

The basic protocol examining the effects of Ca^{2+} waves on bAP evoked $[Ca^{2+}]_i$ changes is shown in Figure 1. A pair of bAPs was evoked with brief intrasomatic pulses. These bAPs generated transient $[Ca^{2+}]_i$ increases at all dendritic locations in the field of view (~100 μm in most experiments). These changes are shown both as a signal from a single ROI and as a pseudo line scan display. In the first experiment a Ca^{2+} wave was generated in the dendrites with tetanic synaptic stimulation (100 Hz for 1 s; Nakamura *et al.* 1999) in the interval between the two bAPs. In this case the amplitude of the second bAP evoked $[Ca^{2+}]_i$ increase, measured at a site where the Ca^{2+} wave was generated, was less than the signal from the first bAP. In the next trial ("no priming") the same tetanus did not evoke a Ca^{2+} wave and there was no reduction in the bAP $[Ca^{2+}]_i$ increase. The failure to generate a Ca^{2+} wave in this trial was probably due to the emptying of the Ca^{2+} stores by the Ca^{2+} wave in the first trial (Miller *et al.* 1996; Hong & Ross, 2007). Consistent with this interpretation, when the cell was primed with a train of bAPs (1 Hz for 1 min) the same synaptic tetanus generated a Ca^{2+} wave and suppressed the amplitude for the second bAP signal. The failure to suppress the bAP signal when the Ca^{2+} wave was not generated suggests that the Ca^{2+} wave was responsible for the suppression and not other pathways activated by the synaptic tetanus (e.g. mGluRs, PLCβ, PKC, DAG).

To further test this conclusion we generated a Ca^{2+} wave by uncaging IP_3 in the dendrites (Manita & Ross, 2010). This approach bypasses the molecular components of the Ca^{2+} release process before the IP_3 receptor. This uncaging evoked Ca^{2+} wave also suppressed the bAP generated $[Ca^{2+}]_i$ increase (Fig. 1B). The summary statistics (Fig. 1C) show that the suppressed amplitude was typically 60-70% of the first spike signal, measured at a site near the center of the Ca^{2+} wave (synaptically induced: 68.0 ± 2.1% and uncaging induced: 61.0 ± 2.4%, compared with the peak amplitude of bAP evoked $[Ca^{2+}]_i$ increase before the Ca^{2+} wave). The similarity of the Ca^{2+} waves and the resulting suppression from the two ways of doing the experiments (synaptic stimulation or uncaging IP_3) also suggested that in some experiments we could use uncaging to

quantitatively assay the suppression. With uncaging, we could more reproducibly generate Ca^{2+} waves and control their spatial and temporal characteristics.

One possible mechanism for the suppression is that the Ca^{2+} wave affected the peak membrane potential amplitude of the spike, reducing the amount of Ca^{2+} entry through voltage-gated Ca^{2+} channels (VGCCs). The expanded electrical traces (Fig. 1B) show that the somatically recorded APs were unaffected by the dendritic Ca^{2+} wave. To more directly test this possibility we repeated these experiments with patch recordings at the sites of wave generation. Figure 2A shows an example where a Ca^{2+} wave in the dendrites did not affect the AP amplitude or shape at the recording site but did suppress the $[Ca^{2+}]_i$ increase (spike fluorescence signal ratio, 0.70±0.04, spike amplitude ratio, 1.01±0.02, n=4; Fig. 2B). Similarly, a Ca^{2+} wave generated by an uncaging flash to the soma suppressed the AP signal but did not affect the electrical recording from the cell body (data not shown). Another possibility is that the large $[Ca^{2+}]_i$ increase from the Ca^{2+} wave activated a K^+ conductance, which persisted until the second bAP and affected the spike parameters. However, 100 nM apamin, which blocks SK channels (the dominant K^+ channel activated by Ca^{2+} waves; Hong *et al.* 2007; El-Hassar *et al*. 2011) did not affect the Ca^{2+} wave mediated suppression or the spike parameters (Control: fluorescence signal ratio, 0.66±0.05, spike width ratio, 0.98±0.04, spike amplitude ratio, 1.01±0.01; 100 nM apamin, fluorescence signal ratio, 0.70±0.07, spike width ratio, 1.04±0.02, spike amplitude ratio, 1.00±0.01, n=4; Fig. 2C). These experiments show that the suppression mechanism affected the VGCCs opened by the bAP and not the peak bAP amplitude or width.

If the suppression is caused by the $[Ca^{2+}]_i$ increase of the Ca^{2+} wave then we would expect the suppression to be largest where the wave is generated and less at other locations. The experiments in Figure 3 confirm this idea. In one cell (Fig. 3A) sites near the center of the wave (green and blue ROIs) showed the greatest suppression and sites at the edge of the wave (red and magenta ROIs) showed no suppression. A detailed profile along the dendrite of another cell (Fig. 3B) confirms that the suppression was maximal at the center of the wave. The experiments supply additional evidence that the Ca^{2+} waves did not affect the electrical properties of the bAP since there was no suppression at sites distal to the Ca^{2+} wave.

These experiments suggest that the suppression is proportional to the magnitude of the $[Ca^{2+}]_i$ increase generated by the wave. Figure 3C shows data from many cells where we compared these two parameters. The $[Ca^{2+}]_i$ increase was measured using the low affinity indicator OGB-5N ($K_d \sim 20\mu M$; Molecular Probes catalogue), making the $[Ca^{2+}]_i$ increases proportional to the fluorescence signal ($\Delta F/F$). These increases were normalized to the signal from a single bAP (evoked before the wave) at the same location. This normalization facilitated comparison among cells. Although there was scatter, the figure supports the hypothesis of proportionality. Grouping the data into bins (Fig. 3D) confirms the significance of the trend.

In most of these experiments we measured the suppression about 6 s after the generation of the Ca^{2+} wave. To determine the time window for this effect and to estimate the recovery time we measured the suppression with test bAPs evoked at different times after the Ca^{2+} was generated. We did this experiment in two ways. In one (Fig. 4A) we evoked a train of bAPs at 1 s intervals, then generated a Ca^{2+} wave with a UV flash after the third bAP, and measured the amplitudes of the bAP signals over the next 25 s. The suppression was maximal just after the Ca^{2+} wave and recovered to about 80% of the prestimulus amplitude by the end of the trial. The $[Ca^{2+}]_i$ did not completely recover to baseline levels between bAPs in the initial few seconds after the Ca^{2+} wave (Fig. 4B). This "residual" $[Ca^{2+}]_i$ should not depress the transient amplitudes since the response of OGB-1 is almost linear in this range (Fig. 4C). Nevertheless, we usually waited 5 s after the Ca^{2+} wave before making measurements to eliminate this potential problem. The second protocol for measuring the recovery time was to repeat experiments like those in Figure 1 only varying the time before evoking the second bAP. This protocol avoided any potential problems from residual signals from the bAP train in the first approach. Figure 4D (with summary results in Figure 4E) shows that the recovery time was about 30 s, consistent with the results using the first method.

Suppression by NMDA spikes

Since synaptically activated Ca^{2+} waves are generated most strongly on the primary apical dendrite (Nakamura *et al.* 1999, 2002) it was not possible to use these

waves to assay bAP signal suppression on the oblique dendrites. To examine the effects of large $[Ca^{2+}]_i$ increases in this region of the dendrites we used NMDA spikes (Schiller *et al.* 2000), which are often generated by a similar synaptic tetanus. These spikes generate large $[Ca^{2+}]_i$ increases predominantly by regenerative Ca^{2+} entry through NMDA receptors. They have been studied most extensively in the basal dendrites of rat L5 pyramidal neurons (Major *et al.* 2008), but have also been observed on oblique and tuft dendrites (Larkum *et al.* 2009; Antic *et al.* 2010).

Figure 5A shows an experiment where we tested whether these NMDA spikes could suppress bAP Ca^{2+} signals on the oblique dendrites. A synaptic tetanus (100 Hz for 500 ms) evoked a Ca^{2+} wave on the main apical dendrite and a regenerative NMDA spike on an oblique dendrite with no spatial overlap. These are separate events because the addition of 100 μM APV completely blocked the NMDA spike but had no effect on the Ca^{2+} wave (Nakamura *et al.* 2002). The bAP Ca^{2+} signals were suppressed on both the apical and oblique dendrites by these events (Fig. 5C). The NMDA spike was the cause of the suppression on the oblique dendrite since APV prevented the reduction of the bAP $[Ca^{2+}]_i$ increase at that site. The magnitude of the suppression was proportional to the normalized $[Ca^{2+}]_i$ increase at the sites of suppression on the oblique dendrites (Fig. 5D). However, the slope of the proportionality (red line) was different from the slope for the Ca^{2+} wave mediated suppression on the main apical dendrite (Fig. 3C). This difference may be due to a different mixture of Ca^{2+} channel types in the two compartments (Magee & Johnston, 1995; Yasuda *et al.* 2003) or to the longer duration of the NMDA spikes compared to the duration of Ca^{2+} waves (e.g. Fig. 5A). Also, the spike signals on the oblique dendrites may be smaller than the signals on the main apical dendrite because the spike voltage amplitude declines with distance (Spruston *et al.* 1995). This smaller spike signal would make the normalized NMDA spike amplitude appear larger. The peak suppression amplitude and time course of recovery were about the same in the two compartments (Fig. 5E). These experiments show that a large $[Ca^{2+}]_i$ increase, not from a Ca^{2+} wave, can suppress bAP evoked $[Ca^{2+}]_i$ increases. One caveat to this conclusion is that we could not measure directly the spike voltage amplitude on the oblique dendrites, although the similarity to the suppression on the main apical dendrite suggests that we are dealing with the same mechanism.

Suppression by Ca^{2+} entry through VGCCs

If $[Ca^{2+}]_i$ increases from Ca^{2+} waves and from NMDA spikes can each suppress bAP Ca^{2+} signals then, perhaps, $[Ca^{2+}]_i$ increases from other sources could also affect bAP Ca^{2+} signals. To test this hypothesis we generated $[Ca^{2+}]_i$ increases by stimulating trains of bAPs. These spikes generate $[Ca^{2+}]_i$ increases primarily by opening VGCCs (Markram *et al.* 1995; Sabatini *et al.* 2002). Figures 6A-C show that both trains of bAPs at 100 Hz (Fig. 6A) or depolarizing pulses under voltage clamp (-70 to 0 mV for 2 s, Fig. 6B) were both effective in suppressing the Ca^{2+} signals from bAPs ~30 μm from the soma. (The 2nd bAP signal was 83.7 ± 6.7% of the 1st bAP signal following trains of bAPs and 84.3 ± 2.4% following depolarizing pulses.) The magnitude of this suppression was not as great as the suppression generated by Ca^{2+} waves or NMDA spikes, consistent with the observation that these protocols did not generate the large $[Ca^{2+}]_i$ increases evoked by Ca^{2+} waves or NMDA spikes. We confirmed that the source of Ca^{2+} in these experiments was not release from internal stores by repeating them in ACSF containing 1 μM thapsigargin, a blocker of the ER Ca^{2+}-ATPase (Thastrup *et al.* 1990). In this solution the spike train still evoked a large $[Ca^{2+}]_i$ increase and the 2nd spike signal was still suppressed (n=4; data not shown). As a control for the effectiveness of thapsigargin we observed that a Ca^{2+} wave could not be generated and that the recovery time of the spike signal was increased (Markram *et al.* 1995)

Interestingly, the train of bAPs did not suppress the spike evoked $[Ca^{2+}]_i$ increase ~150 μm from the soma (Figs. 6A and C). Ca^{2+} signals at this distance (on both the distal and oblique dendrites) also were not suppressed by trains at 30 Hz or 63 Hz (data not shown). Most likely the lack of suppression at these locations results from the much smaller $[Ca^{2+}]_i$ increase evoked by the train in distal locations. The smaller $[Ca^{2+}]_i$ increase is a consequence of the smaller amplitude of individual bAPs in the dendrites (e.g. Spruston *et al.* 1995) and the frequency dependent propagation failure of later bAPs in a train (Spruston *et al.* 1995; Callaway & Ross, 1995; Tsubokawa & Ross, 1997). Figure 6A shows evidence of this propagation failure since the $[Ca^{2+}]_i$ increase rises to a plateau in the proximal location while there is an initial peak (arrow) that falls to a small

plateau in the distal location. Since it takes several seconds for the dendritic amplitude of bAPs to recover to their initial value following a train (Spruston *et al.* 1995; Jung *et al.* 1997) we measured suppression 6-10 seconds after the end of the train.

If a train of bAPs can suppress the $[Ca^{2+}]_i$ increase by a bAP generated 4 s after the train (Fig. 6A) then it is likely that a short train of bAPs can suppress the $[Ca^{2+}]_i$ signal from a bAP generated immediately after the train, i.e. the Ca^{2+} entry from the last bAP in a train would be less than the Ca^{2+} entry from the first bAP in the train because the Ca^{2+} influx from earlier bAPs suppressed the Ca^{2+} influx from the later bAPs. The data in Figure 6D support this hypothesis. The figure shows results from an experiment like that shown in Figure 1 except two trains of 5 bAPs were evoked instead of single bAPs. The suppression of the signals from 5 bAPs by the Ca^{2+} wave was less than the suppression of the single bAP signals. Our interpretation is that early bAPs in the train suppressed the $[Ca^{2+}]_i$ increase from later bAPs; this suppression then occluded some of the suppression by the Ca^{2+} wave. However, we have no additional evidence to support this hypothesis.

In other experiments we tried to develop a protocol to assay for suppression of bAP evoked $[Ca^{2+}]_i$ increases using caged calcium, which would have allowed testing at all dendritic locations. However, we found that caged calcium buffered the bAP signal to low amplitudes where it could not be measured reliably, so this approach was abandoned.

Suppression of subthreshold Ca^{2+} signals and localized Ca^{2+} release events

All these experiments tested protocols that suppressed the $[Ca^{2+}]_i$ change caused by a bAP. These APs are known to open a variety of VGCCs in the dendrites (e.g. Magee & Johnston, 1995; Williams & Stuart, 2000; Yasuda *et al.* 2003) including some high threshold channels. However, there also is evidence that subthreshold depolarizations can cause $[Ca^{2+}]_i$ increases, primarily by Ca^{2+} entry through an L-type Ca^{2+} channel (Magee *et al.* 1996; Manita & Ross, 2009). These subthreshold depolarization evoked $[Ca^{2+}]_i$ increases also were suppressed by Ca^{2+} waves (Fig. 7). These experiments suggest that the suppression mechanism acts, at least in part, on L-type channels (see below).

A careful examination of the traces in Figure 7A shows small, noise-like transients on the tops of the Ca^{2+} signals. These transients were more frequent when the membrane was depolarized, and were less frequent following the Ca^{2+} wave. These kinds of transients resemble the localized dendritic Ca^{2+} release events we previously described in these neurons (Manita & Ross, 2009). To more carefully examine the effects of Ca^{2+} waves on these events we selected dendrites where they occurred with relatively high frequency. The data in Figures 8A, B show that the frequency and amplitude of these events were suppressed for about 30 s following synaptic generation of a Ca^{2+} wave. This suppression appears to resemble the suppression of the bAP evoked signals described above. However, when we tried to suppress these events by raising $[Ca^{2+}]_i$ with a long, high frequency train of bAPs (100 Hz for 1 s) we found no suppression (Figs. 8C, D). Together these experiments suggest that Ca^{2+} waves suppress the events by a different mechanism, probably by depleting the stores. Suppression of similar Ca^{2+} release events ("sparks") by store depletion has been described in cardiac myocytes (Lukyanenko *et al.* 1999).

Pharmacological insensitivity of suppression

VGCCs can be modulated by a variety of G-protein coupled receptors and by phosphorylation (e.g. Catterall, 2000). They also are regulated by a direct feedback mechanism (Ca^{2+} dependent inactivation; CDI) when $[Ca^{2+}]_i$ is elevated (Brehm & Eckert, 1978; Budde *et al.* 2002; Peterson *et al.* 1999; see Discussion). The proportionality of suppression to the magnitude of the preceding $[Ca^{2+}]_i$ increase (Fig. 3), and the lack of a requirement for receptor activation (Figs. 1B and 6), suggested that CDI might be the dominant mechanism. Nevertheless, we tested for the contribution of some other pathways with a variety of pharmacological experiments. Figure 9A shows a typical experiment. We first recorded the Ca^{2+} wave suppression of the bAP $[Ca^{2+}]_i$ increase induced by uncaging IP_3. The experiment was then repeated with the addition of 5 μM staurosporine (a broad spectrum kinase inhibitor) to the ACSF, with no change in the suppression (Fig. 9B). We found a similar insensitivity to FK-506 (a protein phosphatase 2B inhibitor), KN-62 (a CaM Kinase II inhibitor), H-7 (another protein kinase inhibitor),

and W-7 (an inhibitor of Ca^{2+}-calmodulin-dependent phosphodiesterase and myosin light chain kinase). We also tested the possibility that endocannabinoid signaling might contribute to the suppression by adding AM-251 (a CB1 endocannabinoid receptor antagonist) to the ACSF, but found no change in the suppression (summarized in Figure 9C). The lack of sensitivity to these pharmacological agents is consistent with CDI (see Discussion).

We made an attempt to determine if L-type Ca^{2+} channels were a specific target of the suppression mechanism. We found that incubating the slices in 20 μM nimodipine or 20 μM nifedipine had no effect on the $[Ca^{2+}]_i$ increase from single bAPs or on the suppression of Ca^{2+} signals from single bAPs (n = 5). However, this finding does not eliminate the role of L-type channels since several groups (e.g. Mermelstein *et al.* 2000; Nakamura *et al.* 2000) reported that Ca^{2+} entry during APs is insensitive to these compounds, even though L-type channels are known to be in the membrane. This apparent insensitivity is probably due to the use dependence of these inhibitors (Helton *et al.* 2005). In other experiments we tested the effect of nifedipine (20 μM) on the suppression of subtheshold $[Ca^{2+}]_i$ increases. These signals are generated, in part, by Ca^{2+} entry through L-type channels and are sensitive to nifedipine (Magee *et al.* 1996; Manita & Ross, 2009). However, the magnitude of these signals depends on the balance between Ca^{2+} entry and removal and is not directly interpreted as reflecting Ca^{2+} current. Therefore, we could not develop consistent, interpretable measurements from this protocol.

Enhancement of bAP signaling by Ca^{2+} waves

All the preceding experiments examined suppression of bAP Ca^{2+} transients by Ca^{2+} waves and others sources of large $[Ca^{2+}]_i$ increases. However, we previously showed that bAPs could synergistically enhance the $[Ca^{2+}]_i$ increase generated by mGluR mediated synaptic activation if the bAP occurred within 0.5 s of synaptic stimulation (Nakamura *et al.* 1999; Manita & Ross, 2010; see also Wang *et al.* 2000; Rae *et al.* 2000). This enhancement is primarily due to the coincident activation of the IP_3 receptor by IP_3 and Ca^{2+} (e.g. Bezprozvanny *et al.* 1991). Interestingly, we could see many

examples where both of these effects (suppression and enhancement) occurred at the same time in different locations in the dendrites. One experiment is shown in Figure 10. A synaptic tetanus (100 Hz for 500 ms) generated a Ca^{2+} wave in the dendrites. This wave suppressed the following bAP evoked $[Ca^{2+}]_i$ increase (blue arrow) at a site at the center of the wave (blue ROI). However, at the edges of the wave (orange and green ROIs) the bAP evoked $[Ca^{2+}]_i$ increase was enhanced (orange and green arrows). At a more proximal site (red ROI, about 30 μm from the soma) there was no change in the AP evoked $[Ca^{2+}]_i$ increase. The segregation of the different regions is shown more clearly in the pseudo line scan image. Similar patterns were observed when the Ca^{2+} waves were generated by uncaging IP_3 (data not shown). Our interpretation of the enhancement is that some synaptically mobilized or uncaged IP_3 spread in the dendrites beyond the limits of the regenerative Ca^{2+} wave. This peripheral IP_3 did not cause Ca^{2+} release by itself, but could combine with the Ca^{2+} from the bAP to release a small amount of Ca^{2+}, which supplemented the voltage-gated Ca^{2+} entry from the bAP (see also Figure 4D in Manita & Ross, 2010). In most other experiments (e.g. Fig. 3B) we did not see this enhancement, probably because the 2^{nd} bAP was evoked several seconds after the Ca^{2+} wave, beyond the time window for evoking synergistic Ca^{2+} release.

Discussion

There are two main results from these experiments. First, we found that large synaptically activated $[Ca^{2+}]_i$ increases in the dendrites suppress VGCC Ca^{2+} signaling, generated either by bAPs or subthreshold depolarizations. The suppression was evoked either by Ca^{2+} waves or by NMDA spikes (Schiller *et al.* 2000). The Ca^{2+} wave generated $[Ca^{2+}]_i$ increases, mediated by mGluRs (Nakamura *et al.* 1999) also reduced the frequency and amplitude of spontaneous Ca^{2+} release events (Manita & Ross, 2009). These reductions probably result from depleting the stores supplying the Ca^{2+} for the release events since a comparable $[Ca^{2+}]_i$ increase mediated by Ca^{2+} entry through VGCCs did not affect the localized events. However, we cannot rule out a contribution from the suppression of L-type VGCCs since this pathway affects the frequency of Ca^{2+} release events (Manita & Ross, 2009). We did not examine the effects of NMDA spikes on these events.

The NMDA spikes are generated primarily on the oblique and basal dendrites, while the IP_3 mediated Ca^{2+} waves are generated primarily on the main apical dendrite. Therefore, these two sources of $[Ca^{2+}]_i$ increases are produced in non-overlapping dendritic regions. The generation of the $[Ca^{2+}]_i$ increase by Ca^{2+} waves or by NMDA spikes occurs through entirely different mechanisms. Therefore, it is likely that it is the $[Ca^{2+}]_i$ increase, and not some ancillary signaling pathway, that is responsible for the suppression (see below). Consistent with this conclusion large depolarizing pulses and trains of bAPs (Fig. 6) also caused suppression in some dendritic regions.

Complexity of Ca^{2+} signaling interactions

The second important observation is that there are additional components to the complexity in the interactions among different signaling mechanisms generating or suppressing Ca^{2+} signals in the dendrites. One previously reported example is experiments showing that Ca^{2+} entry through some VGCCs affects NMDA receptor Ca^{2+} entry indirectly by modulating SK-type K^+ channels (Bloodgood & Sabatini, 2007; Faber *et al.* 2005). Also, pairing a single bAP with mGluR mediated synaptic transmission

synergistically enhanced the likelihood of generating a Ca^{2+} wave in the dendrites if the spike occurred within 0.5 s of the synaptic tetanus (Nakamura *et al.* 1999; Manita & Ross, 2010). This synergism is due to the coincident activation of the IP_3 receptor by mGluR mobilized IP_3 and bAP evoked Ca^{2+} entry. We also found that mGluR mediated synaptic transmission and Ca^{2+} entry through L-type Ca^{2+} channels enhanced the frequency of localized Ca^{2+} release events (Manita & Ross, 2009).

In this paper we describe ways in which similar synaptic or voltage stimuli can suppress Ca^{2+} signaling. Whether enhancement or suppression occurs depends, primarily, on whether the stimulation evokes a large or small $[Ca^{2+}]_i$ or IP_3 increase, and sometimes on the spatial organization of the interacting signals. For example, we found (Fig. 10) that synaptic stimulation suppressed the bAP evoked $[Ca^{2+}]_i$ increase at some locations by inactivating Ca^{2+} channels but enhanced the increase at other locations by the synergistic effect of IP_3 and Ca^{2+} when both signals occurred within a time window of 0.5 s (Manita & Ross, 2010).

Mechanism of suppression of bAP evoked $[Ca^{2+}]_i$ increase

There are several clues in our data concerning the mechanism responsible for suppression. The most important is that the suppression was proportional to the magnitude of the $[Ca^{2+}]_i$ increase generated by the Ca^{2+} wave. All ways of raising $[Ca^{2+}]_i$ appeared to be effective, ruling out signaling pathways that are activated only by Ca^{2+} waves, NMDA spikes, or trains of bAPs. Second, the suppression was insensitive to several inhibitors of calmodulin dependent kinases and phosphatases and was insensitive to AM251, a blocker of CB-1 endocannabinoid receptors. Both these properties are consistent with suppression due to Ca^{2+}-dependent inactivation (CDI) of Ca^{2+} channels (Brehm & Eckart, 1978; Imredy & Yue, 1994; Dunlap, 2007; however, see Budde *et al.* 2002). This inactivation, which has been studied intensively at the molecular level, is mediated by calmodulin (Peterson *et al.* 1999; Zühlke *et al.* 1999). The lack of sensitivity to the inhibitors results from the tight binding of calmodulin to Ca^{2+} channels near the pore. CDI occurs in most, but not all, members of the high voltage–activated Ca_v1 and Ca_v2 channels, but is absent in the low voltage–activated Ca_v3 channels (Dunlap, 2007).

One variation in our experiments from many studied forms of CDI is the long recovery time from suppression. We found that suppression persisted for 30-60 s and occasionally longer. Most electrophysiological studies of CDI describe shorter recovery times (Patil *et al.* 1998; Wang & Cohen, 2003; Zühlke *et al.* 1999). However, there are several reports of recovery times that match our experiments (Forsythe, 1998; Lee *et al.* 2000; Zeilhofer *et al.* 2000). The reasons for this variation are not understood.

Other aspects of our experiments also appear to be consistent with this mechanism. First, the suppression was observed in both apical and oblique dendrites, which requires that the targets for suppression are found in these regions. Our experiments did not determine which Ca^{2+} channels respond to the $[Ca^{2+}]_i$ increase. However, previous work (Magee & Johnston, 1995; Westenbroek *et al.* 1990) found that all Ca^{2+} channel types are found in different dendritic regions although they are distributed unevenly. Second, the suppression of subthreshold potential evoked $[Ca^{2+}]_i$ increases appeared to be as strong as the suppression of bAP -evoked $[Ca^{2+}]_i$ increases. Since L-type Ca^{2+} channels are activated near threshold in CA1 pyramidal neurons (Magee *et al.* 1996; Lipscombe *et al.* 2004; Manita & Ross, 2009) and are known targets for CDI (Dunlap, 2007) they are likely participants in this suppression, although we could not definitively make this determination.

Comparison with activity dependent Ca^{2+} channel inactivation in spines

It is interesting to compare our results with those of Yasuda *et al.* (2003). Those investigators examined the depression of bAP evoked $[Ca^{2+}]_i$ increases in the dendrites and spines of oblique processes of CA1 pyramidal neurons caused by trains of bAPs. Using 2-photon microscopy to measure $[Ca^{2+}]_i$ changes they found about 30% depression in spines and no depression in the dendrites at locations that appeared to be more than 100 μm from the soma. The depression in spines lasted at least 30 min, was predominantly due to effects on R-type channels, required Ca^{2+} entry through L-type channels, and required activation of CaM KII since the effect was blocked by KN-62. Spine signal depression measured in Yasuda *et al.* (2003) was dependent on cyclic AMP-

dependent protein kinase (PKA) since it was blocked by bath application of the PKA blocker Rp-cyclic adenosine monophosphorothioate (Rp-cAMPS).

The bAP signal suppression in our experiments has some different characteristics than the depression observed by Yasuda *et al.* (2003), in particular, the lack of pharmacological sensitivity. The most likely source of this difference is that our experiments mainly examined suppression in the primary apical dendrites, while they looked in the more distal and oblique dendrites. We looked in the proximal apical dendrites because Ca^{2+} waves are almost exclusively found in this region (Nakamura *et al*. 2002; see also Fig. 5A), and suppression by Ca^{2+} waves was the initial focus of our investigation. However, the vast majority of spines in pyramidal neurons are on the oblique and distal dendrites (Megias *et al.* 2002). Yasuda *et al.* (2003) found that several pharmacological agents affected suppression in the spines. We did not see these effects in our experiments since our pharmacological analysis was done on Ca^{2+} wave signals on the apical dendrites where there are few spines. The lack of pharmacological effects is reasonable for our experiments since most of our measured suppression was probably due to CDI, which is insensitive to the pharmacological agents. The spine suppression in their experiments was through a different mechanism.

The large $[Ca^{2+}]_i$ change generated by the NMDA spike did cause suppression in the oblique dendrites, and the magnitude of this suppression was proportional to the normalized $[Ca^{2+}]_i$ increase at the sites of suppression. However, we did not do a pharmacological analysis on these NMDA spike signals where the spine effects might have been noticed. It would be difficult to do these experiments since the inhibitors of calmodulin dependent kinases and phosphatases would probably affect the generation of the NMDA spike itself. In addition, it was not possible to generate NMDA spikes of the same magnitude in successive trials, which would be a requirement for this kind of experiment. On the main shaft we could replace synaptic activation of the Ca^{2+} wave with a wave generated by uncaging IP_3. This technique gave reproducible Ca^{2+} waves, which allowed the spike signals to be tested for pharmacological sensitivity.

Even though we were using a camera system that did not resolve spines from dendrites it is possible that we could have detected signs of spine depression on the oblique dendrites in the AP train experiments since spines comprise about 25% of the

total volume of oblique dendrites (Katz *et al.* 2009; Yael Katz, personal communication). Our failure to detect this suppression probably reflects the fact that we were looking at locations with lower spine density, although we have no way of knowing if that was the case in our experiments.

One potential conflict with the results of Yasuda *et al.* (2003) is the suppression caused by a train of bAPs (Fig. 6A). We found suppression in the primary apical dendrites (~30 μm from the soma) while they found no suppression on the dendrites from a comparable train. However, when we looked at distal or oblique dendrites, ~150 μm from the soma, where Yasuda *et al.* (2003) did most of their experiments, we did not detect suppression on the dendrites, consistent with their results. The failure to cause suppression at this distance is probably because of the frequency dependent propagation of bAPs into the dendrites (see Results). As noted above, we did detect suppression on the oblique dendrites from the NMDA spikes, but these spikes caused much larger $[Ca^{2+}]_i$ changes than the train of bAPs at that location (Fig. 5B).

Functional Implications

The suppression of bAP evoked $[Ca^{2+}]_i$ increases we observed could be evoked by several mechanisms. The greatest suppression was induced by the large $[Ca^{2+}]_i$ increases generated by Ca^{2+} waves and NMDA spikes. While these events have not been detected *in vivo* under physiological conditions (possibly because the appropriate experiments have not been performed) they both can be induced in slices with moderate intensity (subthreshold for AP generation) tetanic synaptic stimulation – a protocol which is widely used in synaptic plasticity experiments. In addition, a clear but smaller suppression could be achieved with trains of bAPs, which are similar to bursts sometimes recorded *in vivo* (Hirase *et al.* 2001).

We can divide the potential consequences of the suppression of bAP evoked $[Ca^{2+}]_i$ increases into two components: suppression in spines and suppression in the parent dendrite. Within the spine the suppression may modulate the induction of LTP in the same way that Yasuda *et al.* (2003) previously demonstrated. Since Ca^{2+} waves and NMDA spikes generate substantially larger $[Ca^{2+}]_i$ increases than trains of bAPs this

modulation could be even stronger following protocols that induce these events. However, these consequences remain speculative since we did not observe directly $[Ca^{2+}]_i$ changes in spines.

The possible consequences of suppression in the main dendrites depend on those processes which are controlled by changes in $[Ca^{2+}]_i$ in these regions. One candidate is the generation of endocannabinoids, which acts on nearby interneurons to modulate synaptic inhibition and excitation (reviewed by Regehr *et al.* 2009). DAG lipase, which catalyzes the synthesis of this messenger in a Ca^{2+} dependent manner, is concentrated in the dendrites. Changes in bAP evoked $[Ca^{2+}]_i$ entry should modulate this synthesis. In addition, changes in membrane conductances that respond to $[Ca^{2+}]_i$ increases, like SK and BK type K^+ channels, obviously will be modulated by this suppression.

Author Contributions: SM and WNR designed the experiments; SM, KM, and WNR collected, analyzed and interpreted the data; WNR wrote the paper with contributions from SM and KM.

Acknowledgements: Supported in part by NIH grant NS-016295. We thank Nechama Lasser-Ross for computer programming and discussions.

References

Antic SD, Zhou WL, Moore AR, Short SM & Ikonomu KD (2010). The decade of the dendritic NMDA spike. *J Neurosci Res* **88**,2991-3001.

Bezprozvanny I, Watras J & Ehrlich BE (1991). Bell-shaped calcium-response curves of Ins(1,4,5)P_3- and calcium-gated channels from endoplasmic reticulum of cerebellum. *Nature* **351**,751-754.

Bloodgood BL & Sabatini BL (2007). Nonlinear regulation of unitary synaptic signals by CaV(2.3) voltage-sensitive calcium channels located in dendritic spines. *Neuron* **53**,249-260.

Brager DH & Johnston D (2007). Plasticity of intrinsic excitability during long-term depression is mediated through mGluR-dependent changes in I(h) in hippocampal CA1 pyramidal neurons. *J Neurosci* **27**,13926-13937.

Brehm P & Eckert R (1978). Calcium entry leads to inactivation of calcium channels in Paramecium. *Science* **202**,1203–1206.

Budde T, Meuth S & Pape HC (2002). Calcium-dependent inactivation of neuronal calcium channels. *Nat Rev Neurosci* **3**,873–883.

Callaway JC & Ross WN (1995). Frequency-dependent propagation of sodium action potentials in dendrites of hippocampal CA1 pyramidal neurons. *J Neurophysiol* **74**,1395-1403.

Catterall WA (2000). Structure and regulation of voltage-gated Ca^{2+} channels. *Annu Rev Cell Dev Biol* **16**,521-555.

Dudman JT, Tsay D & Siegelbaum SA (2007). A role for synaptic inputs at distal dendrites: instructive signals for hippocampal long-term plasticity. *Neuron* **56**:866-879.

Dunlap K (2007). Calcium channels are models of self-control. *J Gen Physiol* **129**,379-383.

El-Hassar L, Hagenston AM, D'Angelo LB & Yeckel MF (2011). Metabotropic glutamate receptors regulate hippocampal CA1 pyramidal neuron excitability via Ca^{2+} wave-dependent activation of SK and TRPC channels. *J Physiol* **589,** 3211–3229.

Faber ES, Delaney AJ & Sah P (2005). SK channels regulate excitatory synaptic transmission and plasticity in the lateral amygdala. *Nat Neurosci* **8**,635-641.

Fan Y, Fricker D, Brager DH, Chen X, Lu HC, Chitwood RA & Johnston D (2005). Activity-dependent decrease of excitability in rat hippocampal neurons through increases in I(h). *Nat Neurosci* **8**,1542-1551.

Fernández de Sevilla D, Núñez A, Borde M, Malinow R & Buño W (2008) Cholinergic-mediated IP_3-receptor activation induces long-lasting synaptic enhancement in CA1 pyramidal neurons. *J Neurosci* **28**,1469-1478.

Forsythe ID, Tsujimoto T, Barnes-Davies M, Cuttle MF & Takahashi T (1998). Inactivation of presynaptic calcium current contributes to synaptic depression at a fast central synapse. *Neuron* **20**,797-807.

Frick A, Magee J & Johnston D (2004). LTP is accompanied by an enhanced local excitability of pyramidal neuron dendrites. *Nat Neurosci* **7**,126-135.

Gordon U, Polsky A & Schiller J (2006). Plasticity compartments in basal dendrites of neocortical pyramidal neurons. *J Neurosci* **26**,12717-12726.

Grover LM & Teyler TJ (1990). Two components of long-term potentiation induced by different patterns of afferent activation. *Nature* **347**,477-479.

Hagenston AM, Fitzpatrick JS & Yeckel MF (2008). MGluR-mediated calcium waves that invade the soma regulate firing in layer V medial prefrontal cortical pyramidal neurons. *Cereb Cortex* **18**,407-423.

Helton TD, Xu W & Lipscombe D (2005). Neuronal L-type calcium channels open quickly and are inhibited slowly. *J Neurosci* **25**,10247-10251.

Hirase H, Leinekugel X, Czurko A, Csicsvari J & Buzsaki G (2001). Firing rates of hippocampal neurons are preserved during subsequent sleep episodes and modified by novel awake experience. *Proc Natl Acad Sci U S A* **98**,9386-9390.

Holbro N, Grunditz A & Oertner TG (2009). Differential distribution of endoplasmic reticulum controls metabotropic signaling and plasticity at hippocampal synapses. *Proc Natl Acad Sci U S A* **106**,15055-15060.

Hong M & Ross WN (2007). Priming of intracellular calcium stores in rat CA1 pyramidal neurons. *J Physiol* **584**,75-87.

Hong M, Manita S & Ross WN (2007). Calcium waves generated by uncaging IP3 or synaptic stimulation evoke an apamin-sensitive AHP in the perisomatic region of hippocampal CA1 pyramidal neurons. *Soc Neurosci Abstr* 786.6.

Imredy JP & Yue DT (1994). Mechanism of Ca^{2+}-sensitive inactivation of L-type Ca^{2+} channels. *Neuron* **12**,1301-1318.

Jung HY, Mickus T & Spruston N (1997). Prolonged sodium channel inactivation contributes to dendritic action potential attenuation in hippocampal pyramidal neurons. *J Neurosci* **17**, 6639-6646.

Katz Y, Menon V, Nicholson DA, Geinisman Y, Kath WL & Spruston N (2009). Synapse distribution suggests a two-stage model of dendritic integration in CA1 pyramidal neurons. *Neuron* **63**,171-177.

Kim J, Jung SC, Clemens AM, Petralia RS & Hoffman DA (2007). Regulation of dendritic excitability by activity-dependent trafficking of the A-type K^+ channel subunit Kv4.2 in hippocampal neurons. *Neuron* **54**,933-947.

Larkum ME, Nevian T, Sandler M, Polsky A & Schiller J (2009). Synaptic integration in tuft dendrites of layer 5 pyramidal neurons: a new unifying principle. *Science* **325**,756-760.

Lasser-Ross N, Miyakawa H, Lev-Ram V, Young SR & Ross WN (1991). High time resolution fluorescence imaging with a CCD camera. *J Neurosci Methods* **36**, 253-261.

Lee A, Scheuer T & Catterall WA (2000). Ca^{2+}/calmodulin-dependent facilitation and inactivation of P/Q-type Ca^{2+} channels. *J Neurosci* **20**,6830-6838.

Lipscombe D, Helton TD & Xu W (2004). L-type calcium channels: the low down. *J Neurophysiol* **92**,2633-2641.

Lukyanenko V, Subramanian S, Gyorke I, Wiesner TF & Gyorke S (1999). The role of luminal Ca^{2+} in the generation of Ca^{2+} waves in rat ventricular myocytes. *J Physiol* **518**,173-186.

Magee JC & Johnston D (1995). Characterization of single voltage-gated Na^{+} and Ca^{2+} channels in apical dendrites of rat CA1 pyramidal neurons. *J Physiol* **487**,67-90.

Magee JC, Avery RB, Christie BR & Johnston D (1996). Dihydropyridine-sensitive, voltage-gated Ca^{2+} channels contribute to the resting intracellular Ca^{2+} concentration of hippocampal CA1 pyramidal neurons. *J Neurophysiol* **76**,3460-3470.

Major G, Polsky A, Denk W, Schiller J & Tank DW (2008). Spatiotemporally graded NMDA spike/plateau potentials in basal dendrites of neocortical pyramidal neurons. *J Neurophysiol* **99**,2584-2601.

Malenka RC & Nicoll RA (1999). Long-term potentiation--a decade of progress? *Science* **285**,1870-1874.

Manita S & Ross WN (2009). Synaptic activation and membrane potential changes modulate the frequency of spontaneous elementary Ca^{2+} release events in the dendrites of pyramidal neurons. *J Neurosci* **29**,7833-7845.

Manita S & Ross WN (2010). IP_3 mobilization and diffusion determine the timing window of Ca^{2+} release by synaptic stimulation and a spike in rat CA1 pyramidal cells. *Hippocampus* **20**,524-539.

Markram H, Helm PJ & Sakmann B (1995). Dendritic calcium transients evoked by single back-propagating action potentials in rat neocortical pyramidal neurons. *J Physiol* **485,** 1–20.

Megías M, Emri Z, Freund TF & Gulyás AI (2001). Total number and distribution of inhibitory and excitatory synapses on hippocampal CA1 pyramidal cells. *Neuroscience* **102**, 527-540.

Mermelstein PG, Bito H, Deisseroth K & Tsien RW (2000). Critical dependence of cAMP response element-binding protein phosphorylation on L-type calcium channels supports a selective response to EPSPs in preference to action potentials. *J Neurosci* **20**,266-273.

Miller LD, Petrozzino JJ, Golarai G & Connor JA (1996). Ca^{2+} release from intracellular stores induced by afferent stimulation of CA3 pyramidal neurons in hippocampal slices. *J Neurophysiol* **76**,554-562.

Nakamura T, Barbara JG, Nakamura K & Ross WN (1999). Synergistic release of Ca^{2+} from IP_3-sensitive stores evoked by synaptic activation of mGluRs paired with backpropagating action potentials. *Neuron* **24**,727-737.

Nakamura T, Nakamura K, Lasser-Ross N, Barbara JG, Sandler VM & Ross WN (2000). Inositol 1,4,5-trisphosphate (IP_3)-mediated Ca^{2+} release evoked by metabotropic agonists

and backpropagating action potentials in hippocampal CA1 pyramidal neurons. *J Neurosci* **20**,8365-8376.

Nakamura T, Lasser-Ross N, Nakamura K & Ross WN (2002). Spatial segregation and interaction of calcium signalling mechanisms in rat hippocampal CA1 pyramidal neurons. *J Physiol* **543**,465-480.

Patil PG, Brody DL & Yue DT (1998). Preferential closed-state inactivation of neuronal calcium channels. *Neuron* **20**,1027-1038.

Peterson BZ, DeMaria CD, Adelman JP & Yue DT (1999). Calmodulin is the Ca^{2+} sensor for Ca^{2+} -dependent inactivation of L-type calcium channels. *Neuron* **22**,549–558.

Power JM & Sah P (2007). Distribution of IP_3-mediated calcium responses and their role in nuclear signalling in rat basolateral amygdala neurons. *J Physiol* **580**,835-857.

Rae MG, Martin DJ, Collingridge GL & Irving AJ (2000). Role of Ca^{2+} stores in metabotropic L-glutamate receptor-mediated supralinear Ca^{2+} signaling in rat hippocampal neurons. *J Neurosci* **20**,8628-8636.

Regehr WG, Carey MR & Best AR (2009). Activity-dependent regulation of synapses by retrograde messengers. *Neuron* **63**,154-170.

Reyes M & Stanton PK (1996). Induction of hippocampal long-term depression requires release of Ca^{2+} from separate presynaptic and postsynaptic intracellular stores. *J Neurosci* **16**,5951-5960.

Sabatini BL, Maravall M & Svoboda K (2001). Ca^{2+} signaling in dendritic spines. *Curr Opin Neurobiol* **11**,349-356.

Sabatini BL, Oertner TG & Svoboda K (2002). The life cycle of Ca^{2+} ions in dendritic spines. *Neuron* **33,** 439–452.

Sakmann B & Stuart G (1995). Patch-pipette recordings from the soma, dendrites, and axon of neurons in brain slices. In *Single channel recording*, 2nd edn, ed. Sakmann B, Neher E, pp. 199-211. Plenum, New York.

Schiller J, Major G, Koester HJ & Schiller Y (2000). NMDA spikes in basal dendrites of cortical pyramidal neurons. *Nature* **404**,285-289.

Spruston N, Schiller Y, Stuart G & Sakmann B (1995). Activity-dependent action potential invasion and calcium influx into hippocampal CA1 dendrites. *Science* **268**, 297-300.

Taufiq AM, Fujii S, Yamazaki Y, Sasaki H, Kaneko K, Li J, Kato H & Mikoshiba K (2005). Involvement of IP_3 receptors in LTP and LTD induction in guinea pig hippocampal CA1 neurons. *Learn Mem* **12**,594-600.

Thastrup O, Cullen PJ, Drøbak BK, Hanley MR & Dawson AP (1990). Thapsigargin, a tumor promoter, discharges intracellular Ca^{2+} stores by specific inhibition of the endoplasmic reticulum Ca^{2+}-ATPase. *Proc Natl Acad Sci U S A* **87,** 2466–2470.

Topolnik L, Chamberland S, Pelletier JG, Ran I & Lacaille JC (2009). Activity-dependent compartmentalized regulation of dendritic Ca^{2+} signaling in hippocampal interneurons. *J Neurosci* **29**,4658-4663.

Tsubokawa H & Ross WN (1997). Muscarinic modulation of spike backpropagation in the apical dendrites of hippocampal CA1 pyramidal neurons. *J Neurosci* **17**, 5782-5791.

Wang HS & Cohen IS (2003). Calcium channel heterogeneity in canine left ventricular myocytes. *J Physiol* **547**,825-833.

Wang SS, Denk W & Häusser M (2000). Coincidence detection in single dendritic spines mediated by calcium release. *Nat Neurosci* **3**,1266-1273.

Westenbroek RE, Ahlijanian MK & Catterall WA (1990). Clustering of L-type Ca^{2+} channels at the base of major dendrites in hippocampal pyramidal neurons. *Nature* **347**,281-284.

Williams SR & Stuart GJ (2000). Action potential backpropagation and somato-dendritic distribution of ion channels in thalamocortical neurons. *J Neurosci* **20**,1307-1317.

Yasuda R, Sabatini BL & Svoboda K (2003). Plasticity of calcium channels in dendritic spines. *Nat Neurosci* **6**,948-955.

Zeilhofer HU, Blank NM, Neuhuber WL & Swandulla D (2000). Calcium-dependent inactivation of neuronal calcium channel currents is independent of calcineurin. *Neuroscience* **95**,235-241.

Zühlke RD, Pitt GS, Deisseroth K, Tsien RW & Reuter H (1999). Calmodulin supports both inactivation and facilitation of L-type calcium channels. *Nature* **399**,159–162.

Figure Legends

Figure 1. Ca^{2+} waves suppress the amplitude of bAP evoked dendritic $[Ca^{2+}]_i$ changes

A, The image (top, right) shows a pyramidal neuron filled with 50 μM OGB-1 from the patch electrode on the soma; the position of the stimulating electrode is indicated with dotted lines. The greyscale image (top, left) shows the spatial profile of the $[Ca^{2+}]_i$ changes along the chain of pixels on the cell image. Two bAPs, 6 s apart, were evoked by 1 ms intrasomatic pulses; between the bAPs a synaptic tetanus (100 Hz for 1 s) evoked a Ca^{2+} wave. The traces (middle) show the $[Ca^{2+}]_i$ changes from the bAPs and Ca^{2+} wave at the black ROI in the top right image. The amplitude of the 2^{nd} bAP signal was smaller than the 1^{st}. Note that the Ca^{2+} wave is localized in the dendrites while the bAP signals are detected over the full dendritic field. When the experiment was repeated ("no priming") with the same intensity tetanus no Ca^{2+} wave was generated and the amplitudes of the bAP signals were the same. The experiment was repeated after priming the stores with a train of bAPs at 1 Hz for 1 min. This time a Ca^{2+} wave again was generated and the bAP signal was suppressed. Membrane potential changes (bottom) were recorded from soma. *B,* A similar experiment except a 500 ms duration, 15 μm diameter, uncaging flash (grey circle on the top right image) was directed at the dendrites 2 s after the first bAP. The patch pipette contained 200 μM caged IP_3. A large Ca^{2+} wave was generated and the amplitude of the second bAP evoked $[Ca^{2+}]_i$ change was reduced. When there was no uncaging pulse the bAP fluorescence amplitudes were the same. There is a brief uncaging artifact at the time of the UV pulse. The bAP evoked $[Ca^{2+}]_i$ changes on the dendrite and electrical recordings on the soma are shown in greater detail to the bottom right. Each pair of electrical recordings shows the first AP (solid line) and the second AP (dashed line). In both cases the APs were identical. *C,* Summary histogram showing the effects of different stimulation paradigms on the bAP evoked $[Ca^{2+}]_i$ changes. Uncaging evoked or synaptically evoked Ca^{2+} waves strongly reduced the 2^{nd} $[Ca^{2+}]_i$ change. Synaptic stimulation that did not evoke a Ca^{2+} wave did not suppress the bAP signal.

Application of the UV flash in cells without caged IP_3 did not suppress the bAP signal. The numbers in parentheses above the bars indicate the number of experiments.

Figure 2. The reduction in bAP evoked $[Ca^{2+}]_i$ increase is not due to a change in the AP peak amplitude or width at the site of the measurement

A, The image shows a dendrite with a patch electrode about 70µm from the soma. The uncaging pulses at that location caused a reduction in the bAP Ca^{2+} signal at the site of the evoked Ca^{2+} wave (solid ROI, **a**) but not at a distal location (dotted ROI, **b**) where the wave did not reach. The inset in the electrical trace shows that there was no change in the AP peak amplitude or shape. The cell was loaded with 50 µM OGB-1. *B,* Summary histogram (*, $p<0.01$; two-tailed t-test; N = 4). *C,* Summary histogram for experiments showing that 100 nM apamin did not affect synaptically evoked Ca^{2+} wave mediated suppression or spike parameters (*, $p<0.01$ for control; *, $p<0.01$ for apamin; two-tailed t-test; N = 4). Ca^{2+} measurements from dendrites; electrical measurements from soma.

Figure 3. The reduction in the bAP evoked $[Ca^{2+}]_i$ increase is greatest at locations with the largest wave generated $[Ca^{2+}]_i$ increase

A, Typical experiment measuring reduction in bAP evoked $[Ca^{2+}]_i$ increase following a synaptically evoked Ca^{2+} wave. The largest reductions (red arrows) were at the blue and green ROIs at the center of the wave. Indicator, 200µM OGB-5N. *B,* Detailed profile (red trace) of the signal suppression (percent of bAP signal at each location) along the dendrite (different cell) showing greatest effect where the wave evoked $[Ca^{2+}]_i$ increase was largest. *C,* Summary of data from 8 cells. The amplitude of the $[Ca^{2+}]_i$ increase from the wave at a specific location was normalized to the amplitude of the bAP signal evoked at that location before the wave was generated. Several locations were chosen for each cell. Larger reductions were measured at locations with the largest wave generated $[Ca^{2+}]_i$ increases. The red line is the best fit to the data, with the line forced to 1.0 when the $[Ca^{2+}]_i$ change was 0. *D,* The same data grouped into two bins showing that the suppression was significantly greater for larger $[Ca^{2+}]_i$ changes.

Figure 4. The reduction in the bAP evoked $[Ca^{2+}]_i$ increase can be detected for 30-60 s after the Ca^{2+} wave

A, bAPs were evoked at 1 Hz and the $[Ca^{2+}]_i$ increases were measured at a location in the dendrites. After the third bAP a UV flash evoked a Ca^{2+} wave near that location and the amplitude of the bAP signals was suppressed for more than 20 s. *B,* The normalized peak amplitude (measured from the base of the transient) and the residual amplitude between bAP signals after the Ca^{2+} wave are plotted. The amplitude was still suppressed at the time the residual amplitude recovered to baseline. *C,* Response to two bAPs, 500 ms apart, measured about 100 μm from the soma. The summated amplitude was always greater (n=5 cells) than the response to the first bAP when there was a residual change from the first bAP. *D,* Overlaid measurements of the bAP evoked $[Ca^{2+}]_i$ increases before and after the Ca^{2+} wave in experiments similar to that in Figure 1. The traces show measurements from an ROI over the dendrites at the center of the wave at 10, 20, 30, and 40 s after the end of the wave. The suppression was strongest at 10s and less at later times. The bottom traces show similar data in experiments where no wave was generated. There was no reduction in the fluorescence signal. *E,* Summary data from many experiments showing strong reduction just after wave generation and no reduction 60s after the wave. Indicator, 50μM OGB-1.

Figure 5. Synaptically evoked NMDA spikes suppress bAP evoked $[Ca^{2+}]_i$ increases on the oblique dendrites

A, An experiment similar to that in Figure 1 except that the low affinity indicator OGB-5N (200 μM) was used. The top part shows ROIs and pseudocolor images of bAP signals and a synaptically evoked (100 Hz for 500 ms, grey vertical bar) Ca^{2+} wave along the main apical dendrite. The lower images show the same experiment except a rectangular ROI and pixel line along an oblique dendrite were selected. The tetanus evoked a larger and slower $[Ca^{2+}]_i$ increase at these locations. Repeating the experiment in the presence of 100 μM APV blocked the large Ca^{2+} signal on the oblique dendrites but had no effect on the Ca^{2+} wave on the apical shaft. *B,* Fluorescence signals at the three ROIs normalized to the amplitude of a bAP signal generated before the tetanus. The wave was about 5X the bAP signal and the NMDA spike more than 15X the bAP signal. *C,* High

resolution measurements showing that the Ca^{2+} wave suppressed the bAP signal on the apical shaft and the NMDA spike suppressed the signal on the oblique dendrite. In the presence of APV the suppression on the oblique dendrite did not occur. *D,* The suppression amplitude was plotted against the $[Ca^{2+}]_i$ increase from the NMDA spike at a specific location, normalized to the amplitude of the bAP signal evoked at that location before the NMDA spike was generated. Larger reductions were measured at locations with the largest normalized NMDA spike generated $[Ca^{2+}]_i$ increases. The red line is the best fit to the data, with the line forced to 1.0 when the $[Ca^{2+}]_i$ change was 0. Only experiments using 200 μM OGB-5N are included in the plot. *E,* Summary (N = 5, NMDA spike; N = 5, Ca^{2+} wave). The time window for the suppression was similar on the oblique dendrites (NMDA spike) and on the apical shaft (Ca^{2+} wave). The amplitude of the bAP evoked transients did not recover to initial values by the end of the 20 s trial. The dotted lines show the amplitudes of a series of bAPs evoked transients at 2 s intervals (normalized to the 1st transient) when there was no Ca^{2+} wave or NMDA spike. In both the apical dendrite (N = 5) and the oblique dendrite (N = 5) there was no change during the 20 s trial, showing that neither indicator bleaching, photodynamic damage, nor change in bAP parameters had an effect on the transients during the trial period.

Figure 6. Ca^{2+} entry through VGCCs suppresses bAP evoked $[Ca^{2+}]_i$ increases

Aa, An experiment similar to the one in Figure 5 except a train of intrasomatically evoked bAPs at 100 Hz was generated instead of a Ca^{2+} wave; the indicator was 50 μM OGB-1 and the 40X lens was used to view a larger field. *Ab,* A reduction in the bAP signal was detected at the dendritic ROI (**a**) 30 μm from the soma, but no change was detected 150 μm from the soma (ROI **b**). Amplitudes were determined by averaging responses 6 – 10 s after the spike train. Note the sharp transient during the train at the distal location (arrow) reflecting frequency dependent spike backpropagation (see text). *B,* A similar experiment using a depolarizing step instead of the bAPs. A 2 s pulse from -70 to 0 mV was generated in voltage clamp mode. The amplitude of the bAP evoked signals was reduced for at least 10 s. For quantitative measurements the signal at a time when the slow baseline recovered to resting level (arrow) was used. *C,* Summary histogram of the experiments. Both the bAP train and the depolarizing pulse significantly suppressed the

bAP signal 30 μm from the soma but there was no suppression from the train 150 μm from the soma ($p<0.05$, two-tailed t-test; N = 13). *D,* Data (open squares and line) from experiments similar to those in Figure 1 except that the control and test conditions were a train of 5 bAPs at 40Hz. The suppression was proportional to the amplitude of the Ca^{2+} wave (normalized to the bAP signal measured at the same location) but not as great as the suppression of the signal from a single bAP (solid squares and line; data from Figure 3C).

Figure 7. Ca^{2+} waves suppress the amplitude of subthreshold $[Ca^{2+}]_i$ increases

A, Two second subthreshold depolarizing pulses (-85 to -55 mV in voltage clamp mode) generated small, persistent $[Ca^{2+}]_i$ increases in the dendrites. Transient changes were detected on the top of the slow $[Ca^{2+}]_i$ increases but not in the trough. Following the second pulse a UV flash (grey circle) generated a Ca^{2+} wave in the dendrites (arrow). The wave strongly reduced the slow signal and the number of transient changes at that location (black ROI) for more than 10 s after the wave. Indicator, 50μM OGB-1. The data (grey traces) were filtered with a 5-point smoothing function (black traces) and the amplitudes of the steps were plotted for control conditions and following the UV flash. *B,* Summary data from 6 cells. The Ca^{2+} wave clearly suppressed the amplitude of the subthreshold response.

Figure 8. Ca^{2+} waves but not trains of bAPs suppress the rate and amplitude of Ca^{2+} release events

A, During a long recording localized $[Ca^{2+}]_i$ increases were detected at one location in the dendrites (black ROI, **b**) but not at a nearby location (grey ROI, **a**). Indicator was 50μM OGB-1. The mean rate and amplitude of the events in a 20s period after the wave was less than before the wave. *B,* Summary histogram of data from 8 experiments showing significant reductions in both parameters. *C,* Similar experiments testing the effect of 100 bAPs at 100 Hz. There was no apparent effect on the rate or amplitude of the spontaneous events. *D,* Summary histogram of data from 6 experiments showing no significant changes in either parameter.

Figure 9. Suppression of bAP evoked Ca^{2+} changes is insensitive to many pharmacological agents

A, Typical experiment. APs were evoked at 1 Hz and the $[Ca^{2+}]_i$ increases were measured at a location in the dendrites. After the third AP a UV flash evoked a Ca^{2+} wave near that location and the amplitude of the bAP signals was suppressed for more than 10 s. The experiment was repeated in the presence of 5μM staurosporine with no clear change in the profile of the Ca^{2+} signals. The amplitude of the Ca^{2+} wave in staurosporine (and in other drugs included in this figure) was within 10% of the amplitude in control conditions. *B,* The normalized peak amplitude was plotted for the both trials. For quantitative measurements amplitudes were determined at 12 s after the wave when the residual amplitude recovered to baseline levels (Fig. 4B). Combined results of experiments on 5 cells showing that the bAP signal amplitude was unaffected by staurosporine at any time. *C,* Summary histogram of experiments testing 7 conditions.

Figure 10. Complex response to the interaction of synaptic stimulation and bAPs

A train of bAPs at 1 Hz was generated with brief intrasomatic pulses. The soma was about 25 μm below the bottom of the cell image. After the 2nd bAP a 100 Hz synaptic tetanus was evoked for 0.5 s. The electrical responses measured with the somatic electrode were subthreshold for AP generation during the tetanus. Near the soma (red ROI) the detected $[Ca^{2+}]_i$ changes (red trace) only showed signals from the bAPs. In the center of the dendrite (blue ROI) a Ca^{2+} wave was generated, which spread about 20 μm in each direction. This wave *suppressed* the amplitude of the bAP signal (blue arrow) that immediately followed the wave. There was no suppression outside the range of the wave. At sites just at the edge of the wave (green and orange ROIs) the bAP signals were *enhanced* (green and orange arrows). Note that neither of these interactions was detected by the electrical recoding on the soma. Typical result for at least 5 cells, but not all cells showed this edge enhancement.

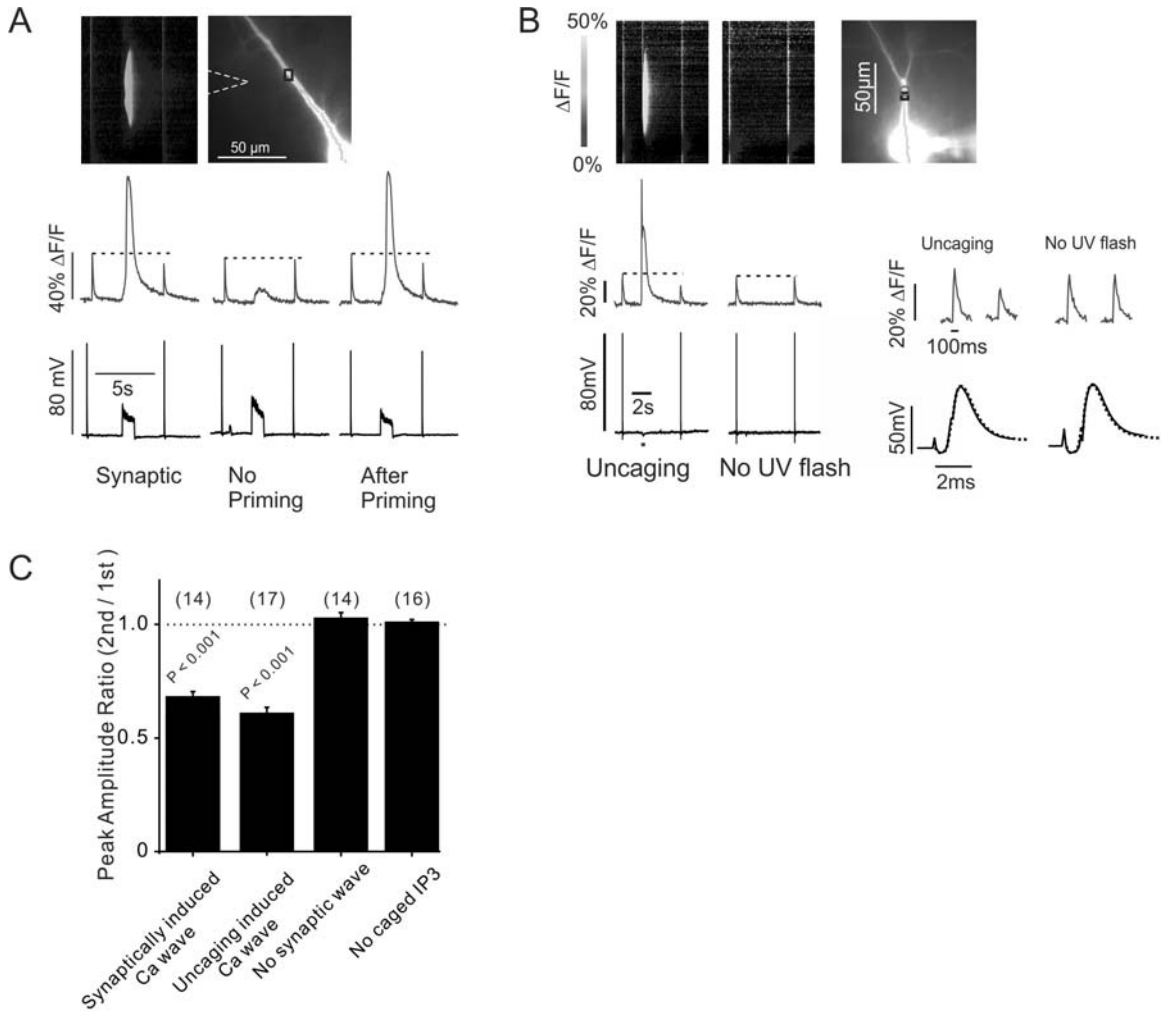
A
50 µm
40% ΔF/F
80 mV
5s
Synaptic
No Priming
After Priming
B
50%
ΔF/F
0%
50µm
20% ΔF/F
80mV
2s
Uncaging
No UV flash
Uncaging
No UV flash
20% ΔF/F
100ms
50mV
2ms
C
Peak Amplitude Ratio (2nd / 1st)
(14)
(17)
(14)
(16)
1.0
0.5
0
P<0.001
P<0.001
Synaptically induced Ca wave
Uncaging induced Ca wave
No synaptic wave
No caged IP3

Figure 1

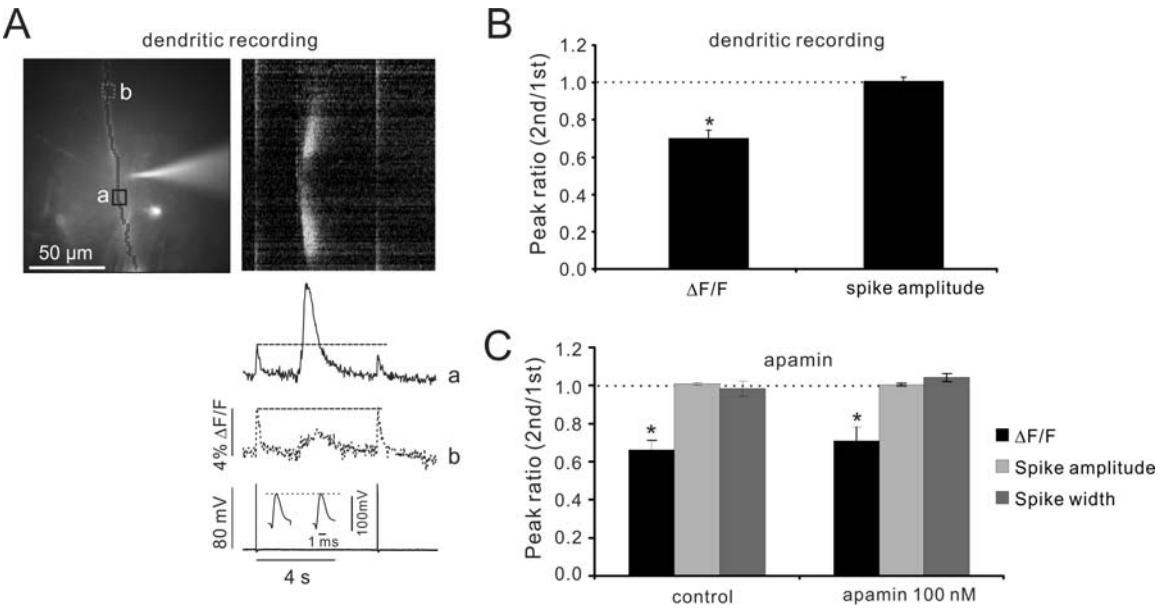
A
dendritic recording
b
a
50 µm
a
4% ΔF/F
b
80 mV
1 ms
100mV
4 s
B
dendritic recording
Peak ratio (2nd/1st)
1.2
1.0
0.8
0.6
0.4
0.2
0.0
*
ΔF/F
spike amplitude
C
apamin
Peak ratio (2nd/1st)
*
*
control
apamin 100 nM
ΔF/F
Spike amplitude
Spike width

Figure 2

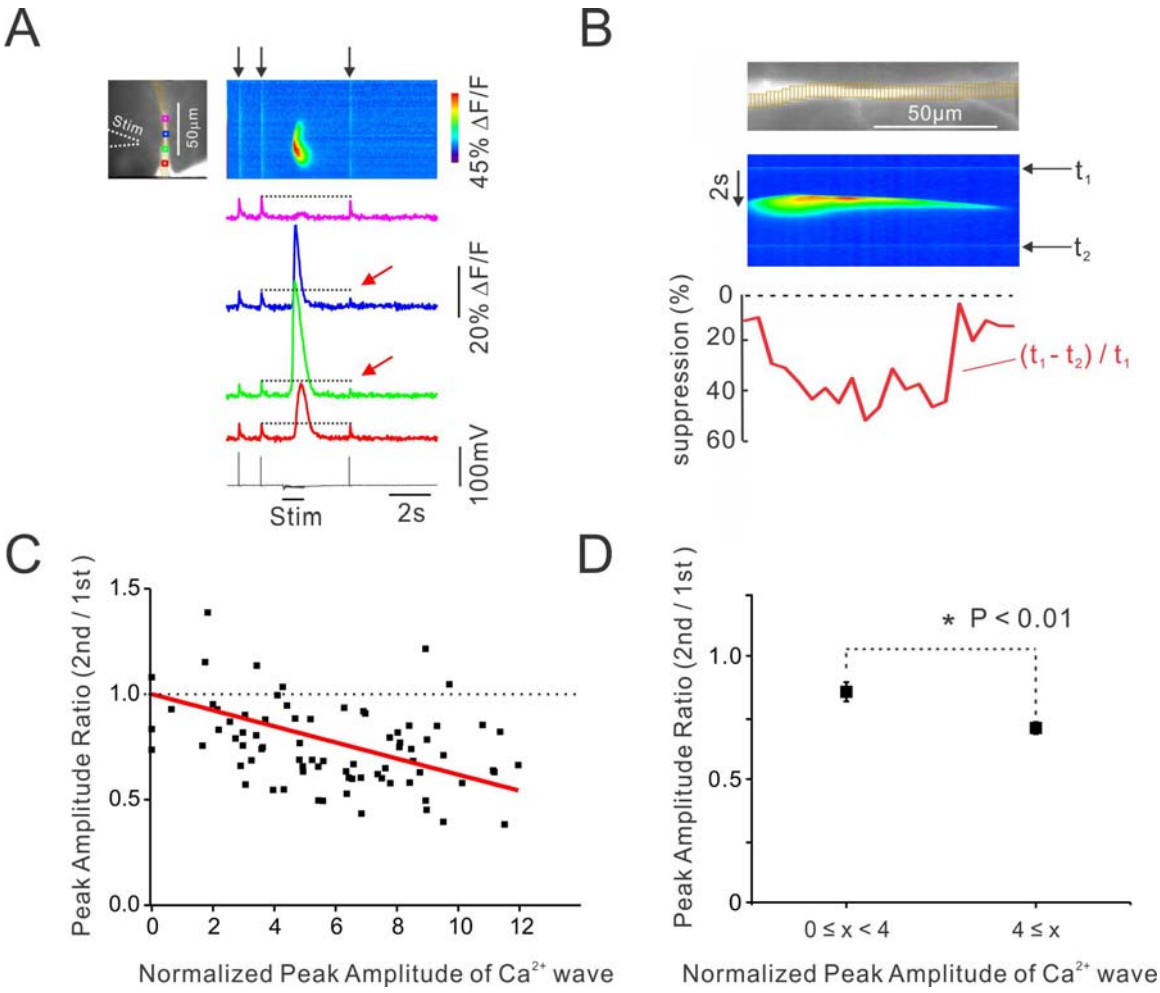
A
Stim
50μm
45% ΔF/F
20% ΔF/F
100mV
Stim
2s
B
50μm
2s
t1
t2
suppression (%)
0
20
40
60
(t1 - t2) / t1
C
Peak Amplitude Ratio (2nd / 1st)
1.5
1.0
0.5
0.0
0
2
4
6
8
10
12
Normalized Peak Amplitude of Ca2+ wave
D
Peak Amplitude Ratio (2nd / 1st)
* P < 0.01
1.0
0.5
0
0 ≤ x < 4
4 ≤ x
Normalized Peak Amplitude of Ca2+ wave

Figure 3

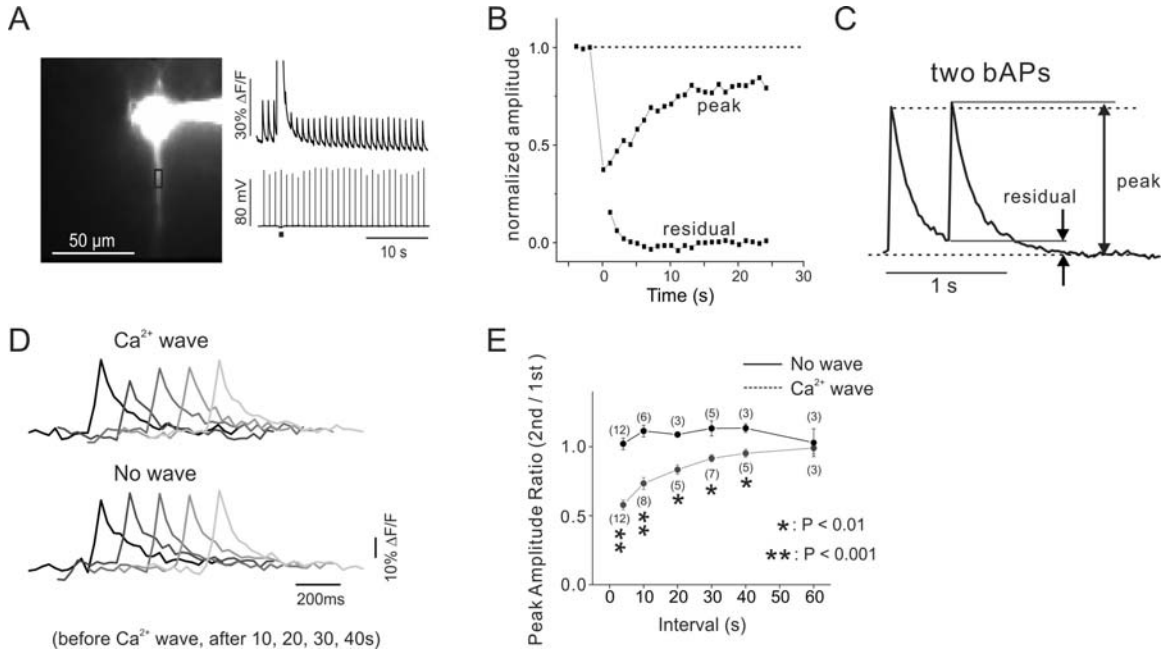
A
50 μm
30% ΔF/F
80 mV
10 s
B
normalized amplitude
peak
residual
Time (s)
C
two bAPs
residual
peak
1 s
D
Ca2+ wave
No wave
10% ΔF/F
200ms
(before Ca2+ wave, after 10, 20, 30, 40s)
E
No wave
Ca2+ wave
Peak Amplitude Ratio (2nd / 1st)
*: P < 0.01
**: P < 0.001
Interval (s)

Figure 4

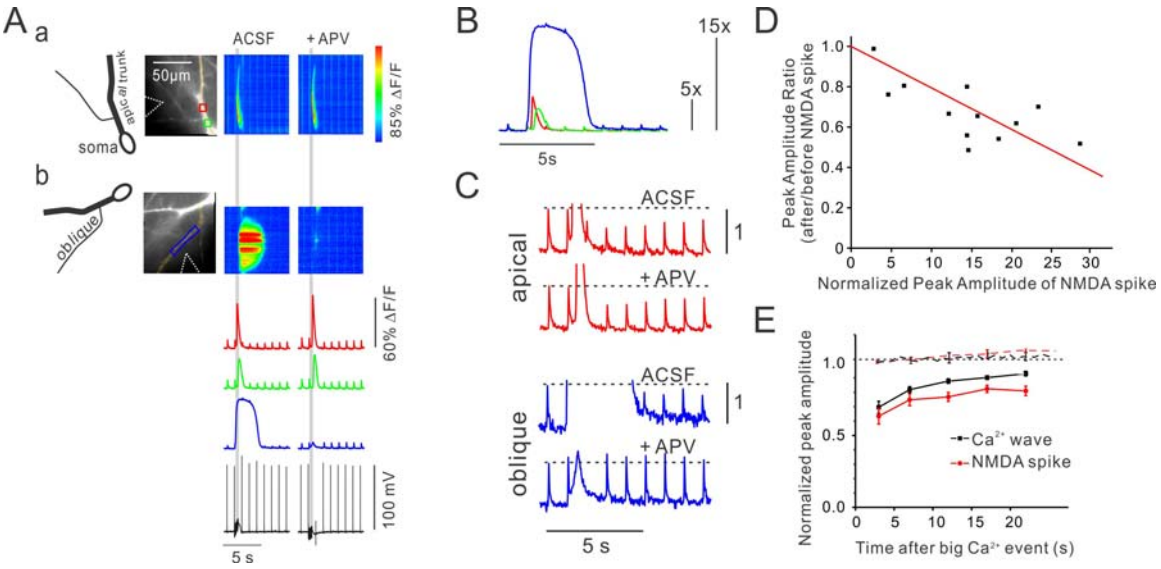
A
a
ACSF
+ APV
50µm
apical trunk
soma
85% ΔF/F
b
oblique
60% ΔF/F
100 mV
5 s
B
15x
5x
5s
C
ACSF
apical
+ APV
1
ACSF
oblique
+ APV
1
5 s
D
Peak Amplitude Ratio (after/before NMDA spike
Normalized Peak Amplitude of NMDA spike
E
Normalized peak amplitude
Ca2+ wave
NMDA spike
Time after big Ca2+ event (s)

Figure 5

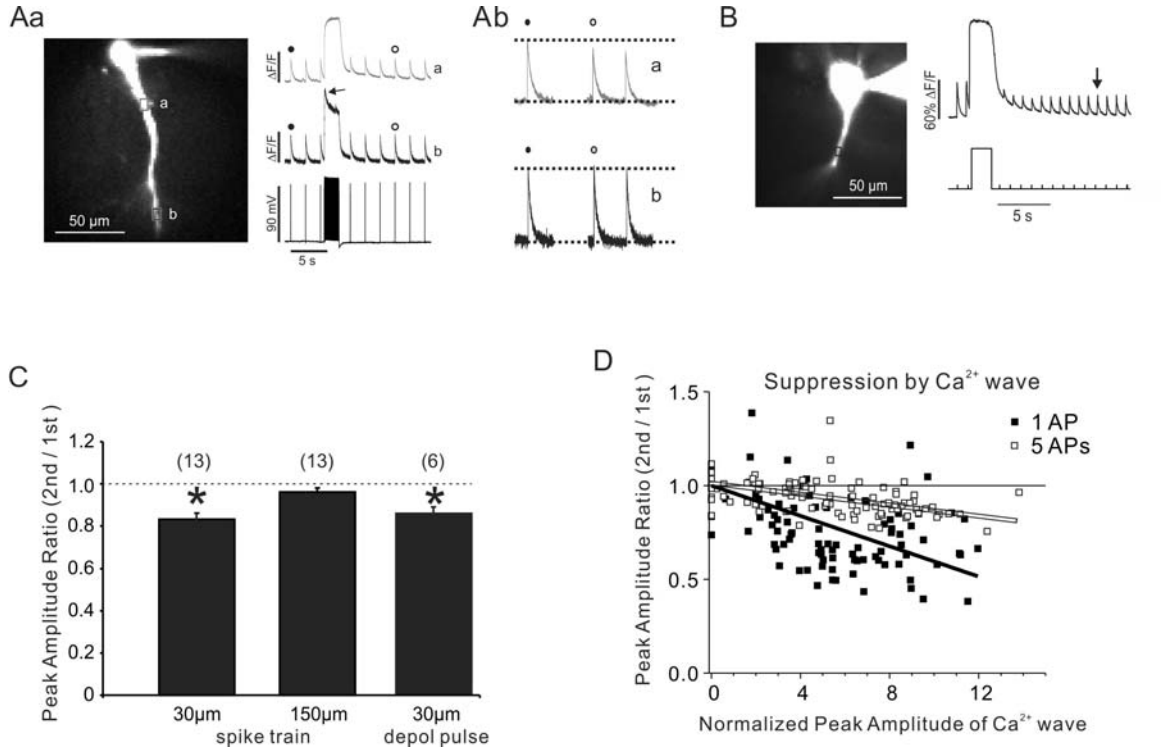
Aa
a
b
50 μm
ΔF/F
a
ΔF/F
b
90 mV
5 s
Ab
a
b
B
50 μm
60% ΔF/F
5 s
C
Peak Amplitude Ratio (2nd / 1st)
1.2
1.0
0.8
0.6
0.4
0.2
0
(13)
(13)
(6)
*
*
30μm
spike train
150μm
30μm
depol pulse
D
Suppression by Ca2+ wave
1 AP
5 APs
Peak Amplitude Ratio (2nd / 1st)
1.5
1.0
0.5
0.0
0
4
8
12
Normalized Peak Amplitude of Ca2+ wave

Figure 6

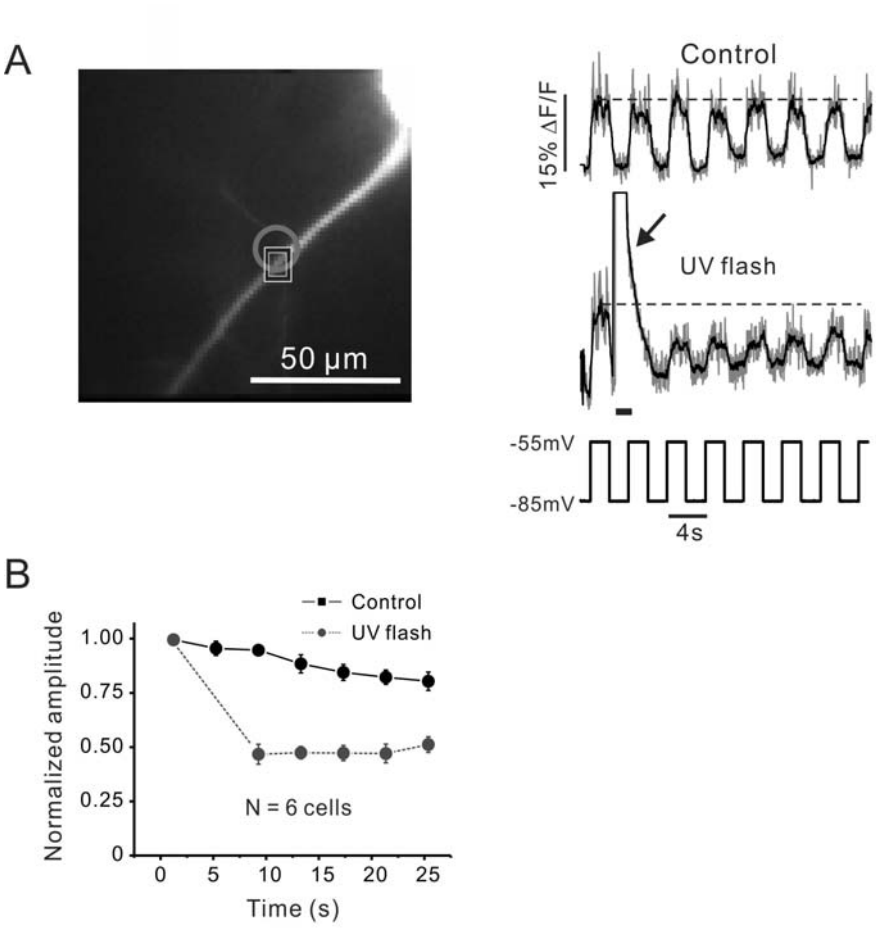
A
50 μm
Control
15% ΔF/F
UV flash
-55mV
-85mV
4s
B
Control
UV flash
Normalized amplitude
1.00
0.75
0.50
0.25
0
N = 6 cells
0
5
10
15
20
25
Time (s)

Figure 7

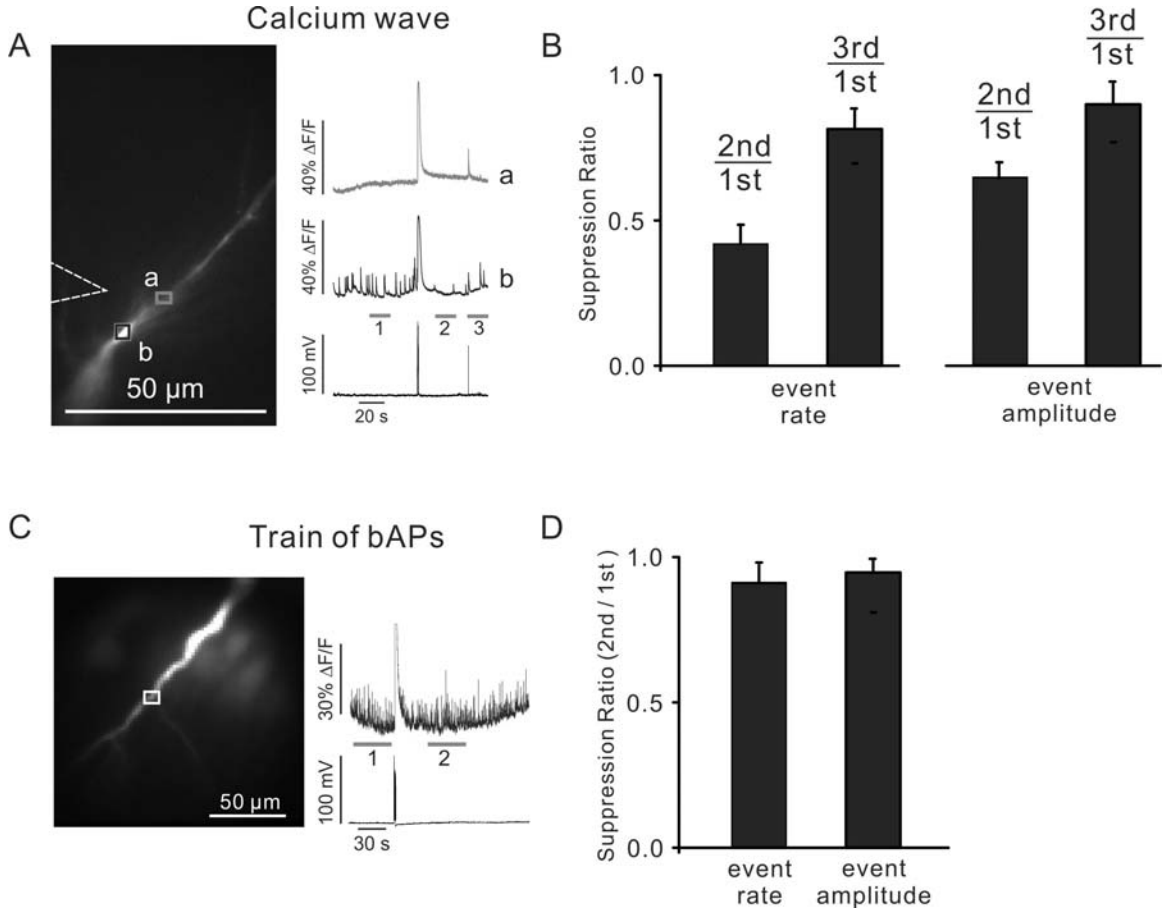
A
Calcium wave
a
b
50 µm
40% ΔF/F
a
40% ΔF/F
b
1
2
3
100 mV
20 s
B
Suppression Ratio
1.0
0.5
0.0
2nd
1st
3rd
1st
2nd
1st
3rd
1st
event
rate
event
amplitude
C
Train of bAPs
50 µm
30% ΔF/F
1
2
100 mV
30 s
D
Suppression Ratio (2nd / 1st)
1.0
0.5
0.0
event
rate
event
amplitude

Figure 8

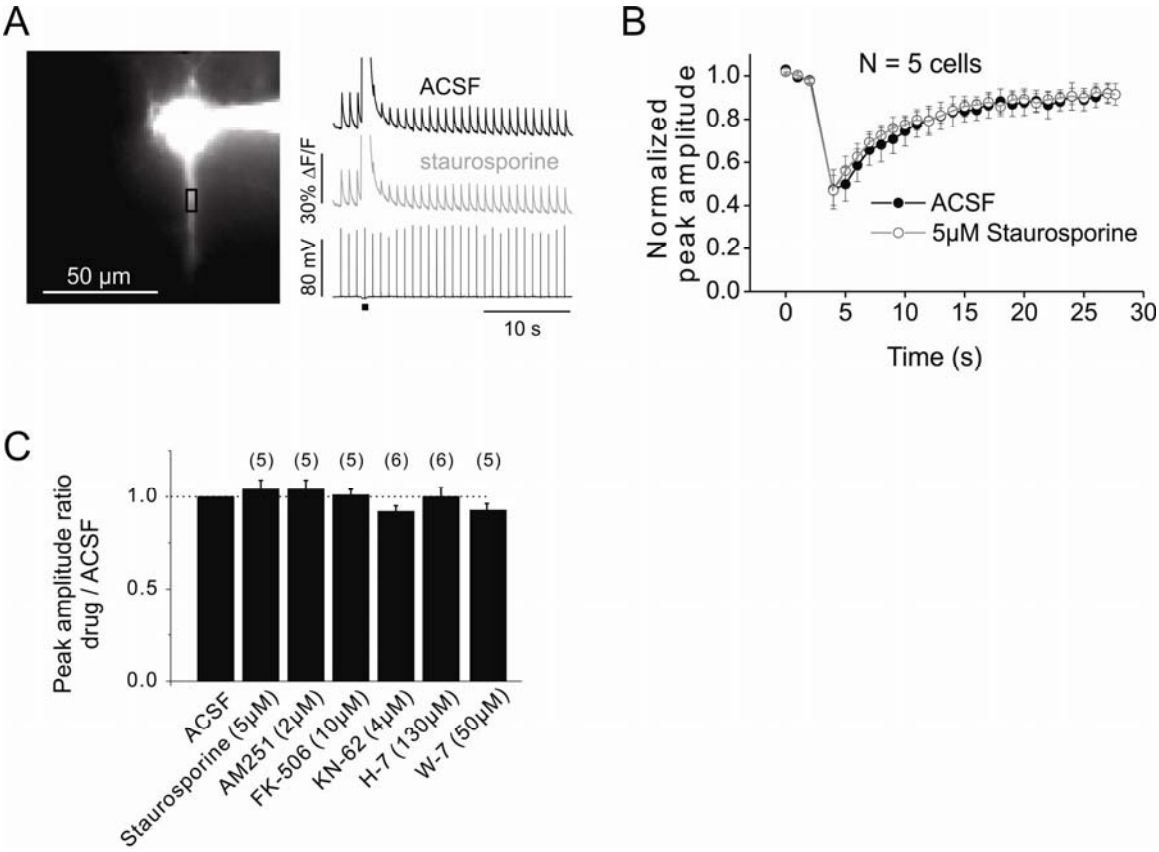
A
50 µm
ACSF
staurosporine
30% ΔF/F
80 mV
10 s
B
N = 5 cells
Normalized peak amplitude
1.0
0.8
0.6
0.4
0.2
0.0
0
5
10
15
20
25
30
Time (s)
ACSF
5µM Staurosporine
C
Peak amplitude ratio drug / ACSF
1.0
0.5
0.0
(5)
(5)
(5)
(6)
(6)
(5)
ACSF
Staurosporine (5µM)
AM251 (2µM)
FK-506 (10µM)
KN-62 (4µM)
H-7 (130µM)
W-7 (50µM)

Figure 9

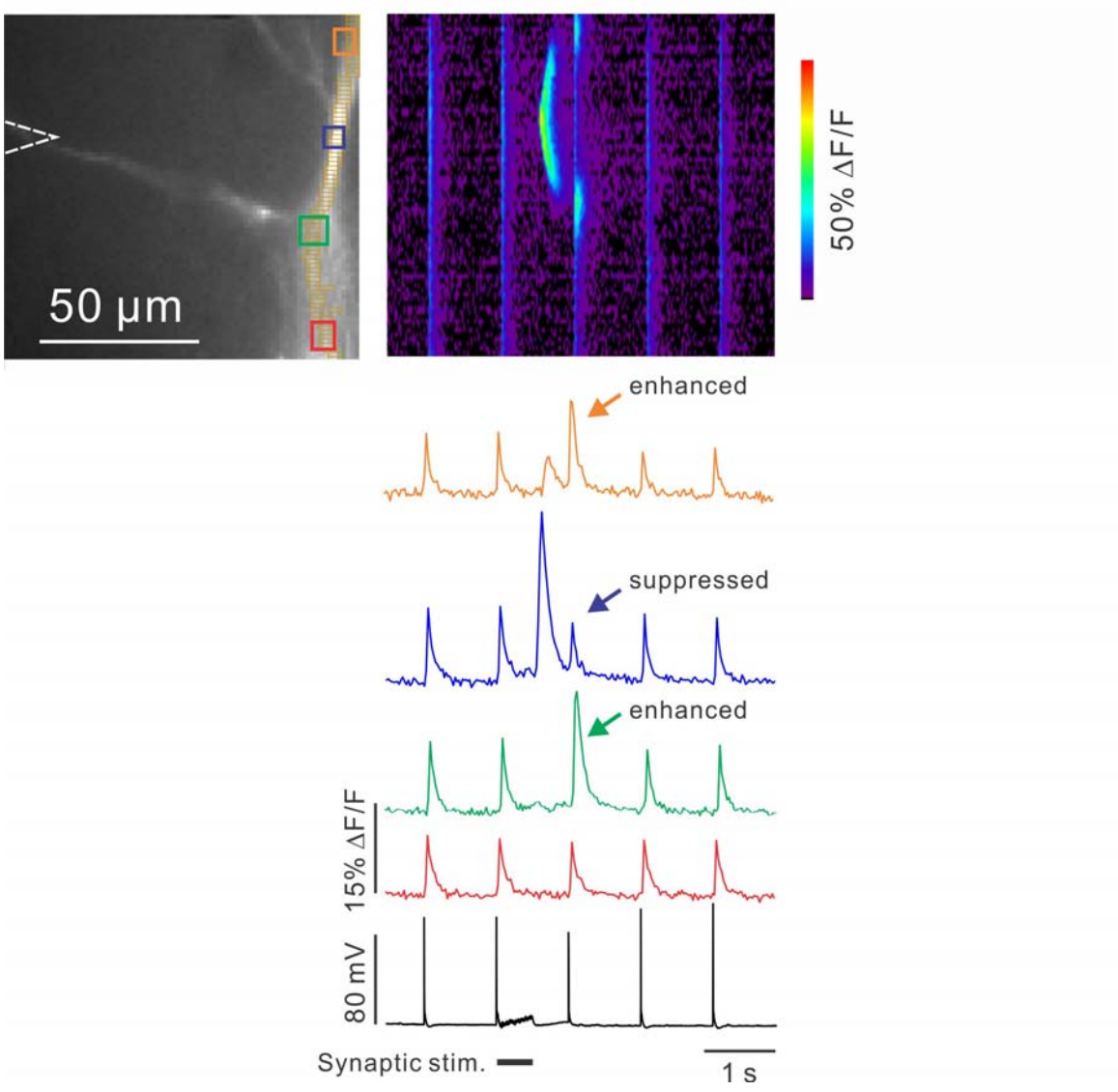
50 µm
50% ΔF/F
enhanced
suppressed
enhanced
15% ΔF/F
80 mV
Synaptic stim.
1 s

Figure 10